

In preparation

2017-09-14; Version 41

Full-length review

The protonmotive force and respiratory control:

Building blocks of mitochondrial physiology

Part 1.

MitoEAGLE Working Group

Corresponding author: E. Gnaiger

Contributing co-authors (*alphabetical, to be extended*):

B. Ahn, M.G. Alves, D.A. Beard, D. Ben-Shachar, S. Breton, G.C. Brown, R.A. Brown, G.R. Buettner, A. Bumsoo, Z. Cervincova, A.J. Chicco, P.M. Coen, J.L. Collins, L. Crisóstomo, M.S. Davis, T. Dias, C. Doerrier, D.A. Fell, A. Filipovska, P.M. Garcia-Roves, L.F. Garcia-Souza, H. Gonzalo, B.H. Goodpaster, D.K. Harrison, K.T. Hellgren, C.L. Hoppel, J. Iglesias-Gonzalez, B.A. Irving, S. Iyer, P. Jansen-Dürr, T. Käämbre, D.A. Kane, T. Komlodi, V. Laner, H.K. Lee, H. Lemieux, E. Lucchinetti, M. Makrecka-Kuka, A.T. Meszaros, N. Moiso, A. Molina, D. Montaigne, A.L. Moore, A.J. Murray, R.K. Porter, K. Nozickova, P.F. Oliveira, P.J. Oliveira, C.M. Palmeira, P.X. Petit, N. Pichaud, E.V. Prochownik, K. Renner-Sattler, J. Rohlena, H.B. Rossiter, D. Salvadego, R. Scatena, M. Schartner, M. Scheibye-Knudsen, G.R. Scott, D. Singer, O. Sobotka, M. Spinazzi, R. Stocker, M. Tanaka, B. Tandler, K. Tepp, K.J. Tronstad, D.J. Tyrrell, B. Velika, M. Vendelin, A.E. Vercesi, Y.H. Wei, M.R. Wieckowski, A. Zorzano

Supporting co-authors (*alphabetical*):

O. Arandarčikaitė, B.M. Bakker, J. Batista Ferreira, P. Bernardi, H.E. Boetker, E. Borsheim, V. Borutaitė, J. Bouitbir, E. Calabria, J.A. Calbet, E. Carvalho, B. Chaurasia, E. Clementi, A. Collin, A.M. Das, C. De Palma, G. Distefano, H. Dubouchaud, M. Duchen, W.J. Durham, S.E. Dyrstad, J. Ehinger, E. Elmer, M. Fornaro, Z. Gan, K.D. Garlid, A. Garten, M.L. Genova, C.W. Gourlay, C. Granata, C.B. Haas, J. Haendeler, J. Han, S.C. Hand, R.T. Hepple, P. Hernansanz, A.J. Hickey, F. Hoel, N.R. Jespersen, H. Kainulainen, G. Keppner, A.V. Khamoui, M. Klingenspor, W.J.H. Koopman, A.J. Kowaltowski, A. Krajcova, R. Kumar Jha, Labieniec-Watala M, G. Lenaz, L.A. MacMillan-Crow, A. Malik, M. Markova, M.A. Menze, A. Methner, J. Muntané, D.M. Muntean, J. Neuzil, S Newsom, D. O'Gorman, M.T. Oliveira, Z. Orynbayeva, Y.K. Pak, H.H. Patel, D. Pesta, I.K.N. Pettersen, S. Pirkmajer, T. Pulinilkunnil, P. Reboredo, M.M. Robinson, E.R. Ropelle, G.V. Røslund, K. Salin, C. Sandi, L.A. Sazanov, J.M. Schilling, K. Siewiera, A.M. Silber, R. Skolik, B.T. Smenes, F.A.A. Soares, I. Sokolova, V.K. Sonkar, P. Stankova, Z. Sumbalova, R.H. Swerdlow, I. Szabo, J.P. Thyfault, A. Towheed, L. Tretter, A. Vieyra, D. Votion, M.-L. Ward, C. Watala, R.C.I. Wust, K.

Zaugg, M. Zaugg

Updates:

http://www.mitoeagle.org/index.php/The_protonmotive_force_and_respiratory_control

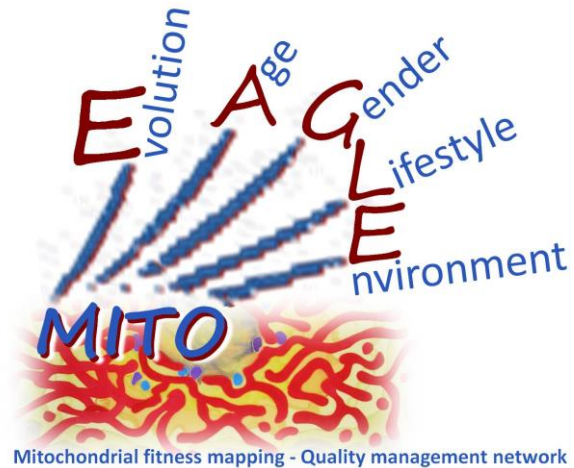
Correspondence: E. Gnaiger

Department of Visceral, Transplant and Thoracic Surgery, D. Swarovski Research Laboratory, Medical University of Innsbruck, Innrain 66/4, A-6020 Innsbruck, Austria

Email: erich.gnaiger@i-med.ac.at

Tel: +43 512 566796, Fax: +43 512 566796 20

This manuscript on 'The protonmotive force and respiratory control' is in preparation as a position statement in the frame of COST Action CA15203 MitoEAGLE. The list of co-authors was initially based on MitoEAGLE Working Group Meetings. In the **bottom-up** spirit of COST, this is an open invitation to scientists and students to join as co-authors, to provide a balanced view on mitochondrial respiratory control, a fundamental introductory presentation of the concept of the protonmotive force, and a critical discussion on reporting data of mitochondrial respiration in terms of metabolic flows and fluxes. We plan a series of follow-up reports by the expanding MitoEAGLE Working Group, to increase the scope of consensus-oriented recommendations and facilitate global communication and collaboration.



It would be great to receive your comments and suggestions by **2017-Sep-18**, particularly if you are an **early career investigator adding an open future-oriented perspective**, or an **established scientist providing a balanced historical basis**. Your critical input into the quality of the manuscript will be most welcome, improving our aims to be educational, general, consensus-oriented, and practically helpful for students working in mitochondrial respiratory physiology.

Please feel free to focus on a particular section in terms of direct input and references, while evaluating the entire scope of the manuscript from the perspective of your expertise.

We organize a MitoEAGLE session linked to our series of reports at the MiPconference Nov 2017 in Hradec Kralove in close association with the MiPsociety (where you hopefully will attend) and at EBEC 2018 in Budapest.

» http://www.mitoeagle.org/index.php/MiP2017_Hradec_Kralove_CZ

I thank you in advance for your feedback.

With best wishes,

Erich Gnaiger

Chair Mitochondrial Physiology Society - <http://www.mitophysiology.org>

Chair COST Action MitoEAGLE - <http://www.mitoeagle.org>

Medical University of Innsbruck, Austria

Contents

1. Introduction

2. Fundamental respiratory coupling states in mitochondrial preparations

2.1. Definitions

Mitochondrial preparations

Respiratory control

Control and regulation

Respiratory control and response

2.2. Three coupling states of mitochondrial preparations and residual oxygen consumption

Coupling states and kinetic control

Pathway control states

Phosphorylation, »P

OXPPOS, ETS, LEAK, ROX

2.3. Classical terminology for isolated mitochondria

States 1-5

2.4. Coupling states and respiratory rates

3. States and rates

3.1. The steady-state

Flux per chamber volume, J_v

3.2. The protonmotive force and proton flow

Faraday constant

Electrical part of the protonmotive force

Chemical part of the protonmotive force

3.3. Forces and flows in physics and irreversible thermodynamics

Vectorial and scalar forces, and fluxes

3.4. Coupling, efficiency, and power

Coupling

Coupled versus bound processes

4. Normalization: flows and fluxes

4.1. Extensive expressions and size-specific normalization

Extensive quantities

Size-specific quantities

Molar quantities

Flow per system, I

Size-specific flux, J

Sample concentration, C_{mX}

Mass-specific flux, J_{mX,O_2}

Number concentration, C_{NX}

Flow per sample entity, I_{X,O_2}

4.2. Normalization for mitochondrial content

Mitochondrial concentration, C_{mte} , and mitochondrial markers

Mitochondria-specific flux, J_{mte,O_2}

4.3. Conversion: oxygen, protons, ATP

5. Conclusions

6. References

Abstract

Clarity of concepts and consistency of nomenclature are trademarks of a research field across its specializations, facilitating transdisciplinary communication and education. As research and knowledge of mitochondrial physiology expand, the necessity for harmonizing nomenclature concerning mitochondrial respiratory states and rates has become apparent. Peter Mitchell's concept of the protonmotive force establishes the link between the electrical and chemical components of energy transformation and its coupling in oxidative phosphorylation. This unifying concept provides the framework for developing a consistent terminology of mitochondrial physiology and bioenergetics. We follow IUPAC guidelines on general terms of physical chemistry, extended by concepts of open systems and irreversible thermodynamics. We align the nomenclature of classical bioenergetics on respiratory states with a concept-driven constructive terminology to address the meaning of each respiratory state. Standards for evaluation of respiratory coupling states must be followed for the development of databases of mitochondrial respiratory function in species, tissues and cells studied under diverse physiological and experimental conditions.

Keywords: Mitochondrial respiratory control, coupling control, mitochondrial preparations, protonmotive force, chemiosmotic theory, oxidative phosphorylation, OXPHOS, efficiency; electron transfer system, ETS; proton leak, LEAK; residual oxygen consumption, ROX; State 2, State 3, State 4; normalization; flow; flux.

- * Does the public expect biologists to understand Darwin's theory of evolution?
- * Do students expect that researchers of bioenergetics can explain Mitchell's theory of chemiosmotic energy transformation?

Mitochondria are dynamic organelles contained within eukaryotic cells, with a double membrane separating an intermembrane space and the matrix with tubular or disk-shaped cristae. Mitochondria were described for the first time in 1857 by Rudolph Albert von Kölliker as granular structures – "sarkosomes". In 1886 Richard Altman called them "bioblasts" (published 1894). The word "Mitochondrium" (Greek mitos: thread; chondros: granule) was introduced by Carl Benda (1898). Mitochondria are the structural and functional elemental units of cell respiration, where cellular respiration is defined as the consumption of oxygen potentially coupled to the physical and chemical processes of ATP production. Mitochondria are the oxygen consuming electrochemical generators. In the process of oxidative phosphorylation (OXPHOS), the reduction of O₂ is electrochemically coupled to conservation of energy in the form of ATP (Mitchell 2011). As part of the OXPHOS system, these powerhouses of the cell contain the coenzyme ubiquinone and cytochrome *b*, *c*, *aa₃* redox systems, and ATP synthase or alternative oxidases, ion transporters including proton pumps, mitochondrial kinases related to energy transfer pathways, the enzymes of the tricarboxylic acid cycle with several dehydrogenases, and the fatty acid oxidation enzymes. The mitochondrial proteome comprises more than 1,200 proteins (Mitocharta), mostly encoded by nuclear DNA (nDNA), with a variety of functions, many of which are relatively well known (*e.g.* apoptotic proteins) or are still under investigation. Mitochondria maintain their own genetic material known as mitochondrial DNA (mtDNA) that encodes 13 peptides and subunits of the transmembrane respiratory Complexes CI, CIII, CIV and CV, and is both regulated and supplemented by nuclear-encoded mitochondrially targeted proteins. There is a constant crosstalk between mitochondria and the other cellular components at the transcriptional or post-translational level, and through cell signalling in

response to varying energy demands. Mitochondrial morphology can change in response to external stimuli via processes known as fusion and fission through which mitochondria can communicate within a network. Abbreviation: mt, as generally used in mtDNA. Mitochondrion is singular and mitochondria is plural. The bioblasts of Richard Altmann (1894) include not only the mitochondria as presently defined, but also symbiotic and free-living bacteria.

‘For the physiologist, mitochondria afforded the first opportunity for an experimental approach to structure-function relationships, in particular those involved in active transport, vectorial metabolism, and metabolic control mechanisms on a subcellular level’ (Ernster and Schatz 1981).

1. Introduction

Every study of mitochondrial function and disease is faced with **E**volution, **A**ge, **G**ender and sex, **L**ifestyle, and **E**nvironment (EAGLE) as essential background conditions characterizing the individual patient or subject, cohort, species, tissue and to some extent even cell line. As a large and highly coordinated group of laboratories and researchers, the global MitoEAGLE Network is uniquely poised to generate the necessary scale, type, and quality of consistent data sets and conditions to address this intrinsic complexity. The MitoEAGLE Working Group aims at developing harmonized experimental protocols and implementing a quality control and data management system to interrelate results obtained in different studies and to generate a rigorously monitored database focused on mitochondrial respiratory function. In this way, workers within the same and across different disciplines will be positioned to compare their findings to an agreed upon set of accepted international standards.

Reliability and comparability of quantitative results depend on the accuracy of measurement under well-defined conditions. A conceptually meaningful framework also is required to relate the results of experiments carried out by different research groups. With an emphasis on

quality of research, data gathered can be useful far beyond the specific question of an experiment. Vague or ambiguous jargon can lead to confusion and may relegate valuable signals to wasteful noise. For this reason, measured values must be expressed in standardized units for each parameter used to define mitochondrial respiratory control. Standardization of nomenclature and technical terms is essential to improve the awareness of the intricate meaning of divergent scientific vocabulary. The MitoEAGLE Network aims at accomplishing the ambitious goal of harmonizing, unifying, and thus simplifying the terminology in the field of mitochondrial physiology. A focus on coupling states in mitochondrial preparations is a first step in the attempt to generate a harmonized and conceptually oriented nomenclature in bioenergetics and mitochondrial physiology. Comparison with coupling states of intact cells (Wagner *et al.* 2011) and respiratory control by fuel substrates and specific inhibitors of respiratory enzymes (Gnaiger 2009; 2014) will be reviewed in subsequent communications.

2. Fundamental respiratory coupling states in mitochondrial preparations

‘Every professional group develops its own technical jargon for talking about matters of critical concern ... People who know a word can share that idea with other members of their group, and a shared vocabulary is part of the glue that holds people together and allows them to create a shared culture’ (Miller 1991).

2.1. Definitions

Mitochondrial preparations are defined as either isolated mitochondria or tissue and cellular preparations in which the barrier function of the plasma membrane is disrupted. In the preparation of isolated mitochondria the cells or tissues are homogenized and the mitochondria are purified from other cell fractions by centrifugation. Mechanical permeabilization is applied in tissue homogenates containing all components of the cell in the crude homogenate. Likewise, in chemically permeabilized tissues or cells the functional integrity and, to a large extent, the structure of mitochondria are maintained. The plasma membrane separates the cytosol, nucleus

and organelles (the intracellular compartment) from the environment of the cell. The plasma membrane consists of a lipid bilayer, embedded proteins and attached organic molecules which collectively control the selective permeability of ions, organic molecules and particles across the cell boundary. The intact plasma membrane, therefore, prevents the passage of many water-soluble mitochondrial substrates, such as succinate or ADP, prohibiting an analysis of respiratory capacity at kinetically saturating [ADP], and thus limiting the scope of investigations into mitochondrial respiratory function in intact cells. The cholesterol content of the plasma membrane is high compared to mitochondrial membranes. Therefore, mild detergents, such as digitonin and saponin, can be applied which selectively permeabilize the plasma membrane by interaction with cholesterol and allow the free exchange of the components of the cytosol with ions and organic molecules of the environment, while the organelles, cytoskeleton and nucleus remain in their intracellular location. Application of optimum concentrations of these mild detergents leads to the complete loss of cell viability, tested by nuclear staining, while mitochondrial function remains unaffected, as shown by the lack of a response of respiration of isolated mitochondria to the addition of such low concentrations of digitonin and saponin. All mitochondria are retained in chemically permeabilized mitochondrial preparations and crude tissue homogenate, whereas a fraction of mitochondria is lost in the process of isolation of mitochondria.

Respiratory control is monitored in a mitochondrial preparation under conditions defined as respiratory states. Coupling states in mitochondrial preparations depend on an exogenous supply of fuel substrates and oxygen. When phosphorylation of ADP to ATP is stimulated or depressed, an increase or decrease is observed in electron flow linked to oxygen consumption in 'controlled' coupling states. Alternatively, coupling of electron transfer with phosphorylation is disengaged by uncouplers, functioning like a clutch in a mechanical system. The corresponding respiratory state is characterized by high levels of oxygen consumption without control by phosphorylation ('uncontrolled state'). Respiratory control refers to the ability of mitochondria

to adjust oxygen consumption in response to external control signals by engaging various mechanisms of control and regulation.

Control and regulation: The terms metabolic *control* and *regulation* are frequently used synonymously, but are distinguished in metabolic control analysis: ‘We could understand the regulation as the mechanism that occurs when a system maintains some variable constant over time, in spite of fluctuations in external conditions (homeostasis of the internal state). On the other hand, metabolic control is the power to change the state of the metabolism in response to an external signal’ (Fell 1997). Respiratory control may be induced by experimental control signals that exert an influence on: (1) ATP demand and ADP phosphorylation rate; (2) fuel substrate, pathway competition and oxygen availability, *e.g.*, starvation and hypoxia; (3) the protonmotive force, redox states, flux-force relationships, coupling and efficiency; (4) Ca^{2+} and other ions including H^+ ; (5) inhibitors, *e.g.*, nitric oxide or intermediary metabolites, such as oxaloacetate. Mechanisms of respiratory control and regulation include adjustments of (1) mitochondrial enzyme activities and allosteric regulation by adenylates, phosphorylation of regulatory enzymes, (2) enzyme content, concentrations of cofactors and conserved moieties (such as adenylates, NAD^+/NADH , coenzyme Q, cytochrome *c*); (3) metabolic channeling by super-complexes; and (4) mitochondrial density (enzyme concentrations and membrane area) and morphology (cristae folding, fission and fusion). Evolutionary or acquired differences in the genetic basis of mitochondrial function (or dysfunction) between subjects and gene therapy; **A**ge; **G**ender and hormone concentrations; **L**ife style including exercise and nutrition; and **E**nvironmental including thermal, toxicological and pharmacological factors (EAGLE) exert an influence on all control mechanisms listed above (for reviews, see Brown 1992; Gnaiger 1993a, 2009; 2014; Morrow *et al.* 2017).

Respiratory control and response: There is a difference between control by a fixed component of a metabolic system or module, *e.g.* ATP synthase, and the response to an experimental variable, *e.g.*, fuel substrate or ADP. Whilst lack of control by a metabolic module, *e.g.*

phosphorylation system, does mean that there will be no response to a variable activating it, *e.g.* [ADP], the reverse is not true; *i.e.*, lack of response to [ADP] does not exclude the phosphorylation system having some degree of control. The degree of control of a component of the OXPHOS system on an output variable of the system, such as oxygen flux, will in general be different from the degree of control on other outputs, such as phosphorylation flux, cytochrome redox states, protonmotive force, phosphorylation potential, proton leak flux (**Table 1**). As such, it is necessary to be specific about which output is being considered. Respiratory control is insufficiently specific in the context of specific interpretations (Fell 1997).

2.2. *Three coupling states of mitochondrial preparations and residual oxygen consumption*

To extend the classical nomenclature (Section 2.3) by a concept-driven terminology that incorporates explicit information on the nature of the respiratory states, the terminology must be general and not restricted to any particular experimental protocol or mitochondrial preparation (Gnaiger 2009). We focus primarily on the conceptual ‘why’, along with clarification of the experimental ‘how’.

Coupling states and kinetic control: In the following section, the concept-driven terminology is explained and coupling states are defined. The capacity of *oxidative phosphorylation*, OXPHOS, provides diagnostic reference values and is, therefore, measured at kinetically saturating concentrations of ADP and inorganic phosphate, P_i . The *oxidative* capacity of the electron transfer system, ETS, reveals the limitation of OXPHOS capacity mediated by the *phosphorylation* system. ETS capacity is measured as noncoupled respiration by application of *external uncouplers*. The contribution of *intrinsically uncoupled* oxygen consumption is most easily studied by not stimulating or arresting phosphorylation, when oxygen consumption compensates mainly for the proton leak; the corresponding states are collectively classified as LEAK states. Coupling states of mitochondrial preparations can be compared in any defined

mitochondrial pathway control state (**Fig. 1**). Fuel substrates and ETS inhibitors are kept constant while (1) adding ADP or P_i , (2) inhibiting the phosphorylation system, and (3) performing uncoupler titrations.

Coupling control states are established in the study of mitochondrial preparations to obtain reference values for various output variables. Physiological conditions *in vivo* may deviate substantially from these experimentally obtained states. Since kinetically saturating concentrations, *e.g.* of ADP or oxygen, may not apply to physiological intracellular conditions, relevant information is obtained in studies of kinetic responses to conditions intermediate between the LEAK state at zero [ADP] and the OXPHOS state at saturating [ADP], or of respiratory capacities in the range between kinetically saturating [O_2] and anoxia (Gnaiger 2001).

Pathway control states are obtained in mitochondrial preparations by depletion of endogenous substrates and addition to the mitochondrial respiration medium of fuel substrates (CHNO) and specific inhibitors, activating selected mitochondrial pathways.

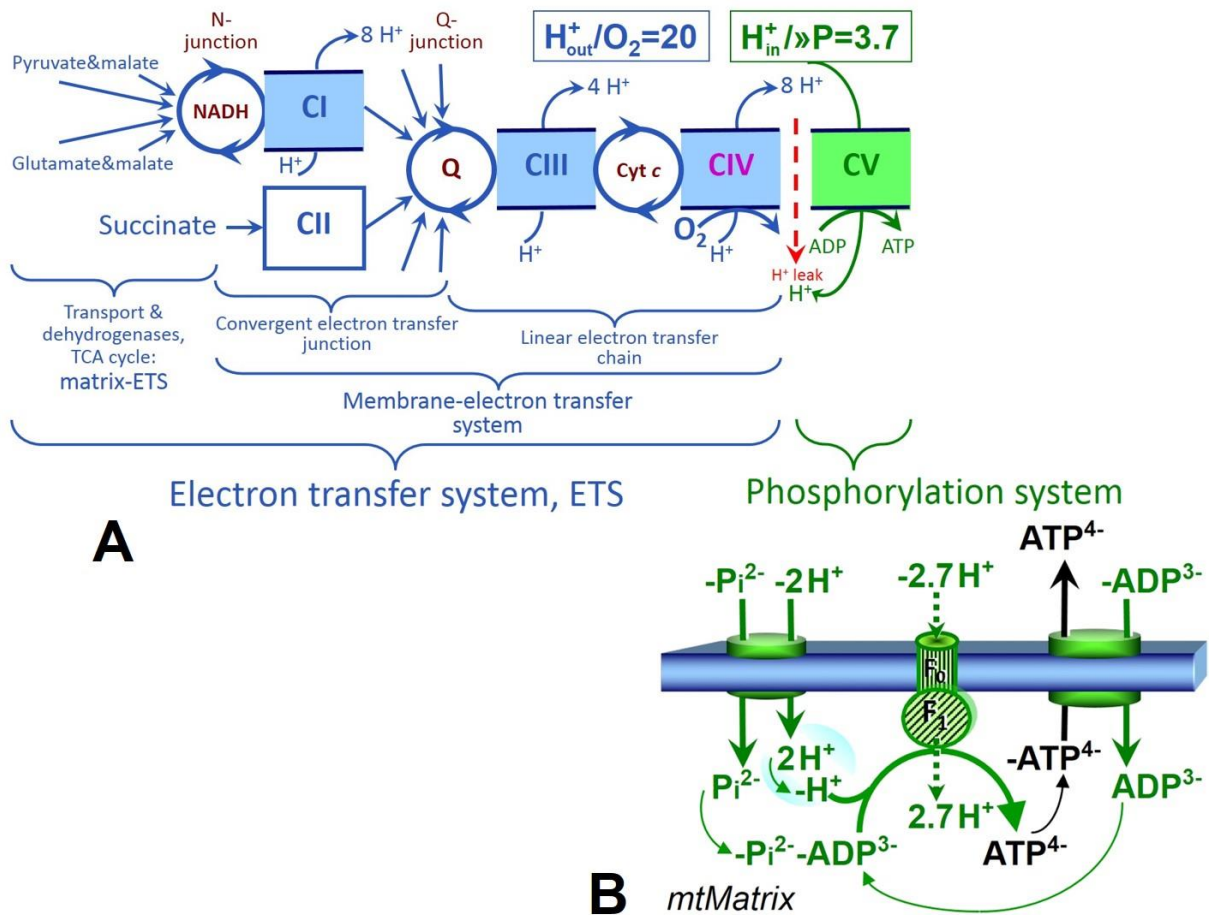


Fig. 1. The mitochondrial respiratory system. In oxidative phosphorylation, the electron transfer system, ETS is coupled to the phosphorylation system. **(A)** Multiple convergent electron transfer pathways are shown from NADH and succinate and additional arrows (electron transferring flavoprotein, glycerophosphate dehydrogenase, and others). H_{out}^+ / O_2 is the ratio of outward proton flux from the matrix space to catabolic O₂ flux in the NADH-linked pathway. $H_{in}^+ / »P$ is the ratio of inward proton flux from the inter-membrane space to the endergonic flux of phosphorylation of ADP to ATP. Due to proton leak and slip these are not fixed stoichiometries. **(B)** The $H_{in}^+ / »P$ stoichiometry is the sum of the coupling stoichiometry in the ATP synthase reaction (-2.7 H⁺ from the intermembrane space, 2.7 H⁺ to the matrix) and the proton balance in the translocation of ADP³⁻, ATP⁴⁻ and P_i²⁻. See Eqs. 11 and 12 for further explanation. Modified from (A) Lemieux *et al.* (2017) and (B) Gnaiger (2014).

Phosphorylation, »P: *Phosphorylation* in the context of OXPHOS is defined as phosphorylation of ADP to ATP. On the other hand, the term phosphorylation is used generally in many different contexts, *e.g.* protein phosphorylation. This justifies consideration of a symbol

more discriminating and specific than P as used in the P/O ratio (phosphate to atomic oxygen ratio), where P indicates phosphorylation of ADP to ATP or GDP to GTP. We propose the symbol »P for the endergonic direction of phosphorylation coupled to catabolic reactions, and likewise the symbol «P for the corresponding exergonic hydrolysis (**Fig. 2**). ATP synthase is the proton pump of the phosphorylation system (**Fig. 1B**). »P may also involve substrate-level phosphorylation as part of the tricarboxylic acid cycle (succinyl-CoA ligase), and phosphorylation of ADP catalysed by phosphoenylpyruvate carboxykinase, adenylate kinase, creatine kinase, hexokinase and nucleoside diphosphate kinase (NDPK). Kinase cycles are involved in intracellular energy transfer and signal transduction for regulation of energy flux. In isolated mammalian mitochondria ATP production catalysed by adenylate kinase, $2\text{ADP} \leftrightarrow \text{ATP} + \text{AMP}$, proceeds without fuel substrates in the presence of ADP (Komlódi and Tretter 2017).

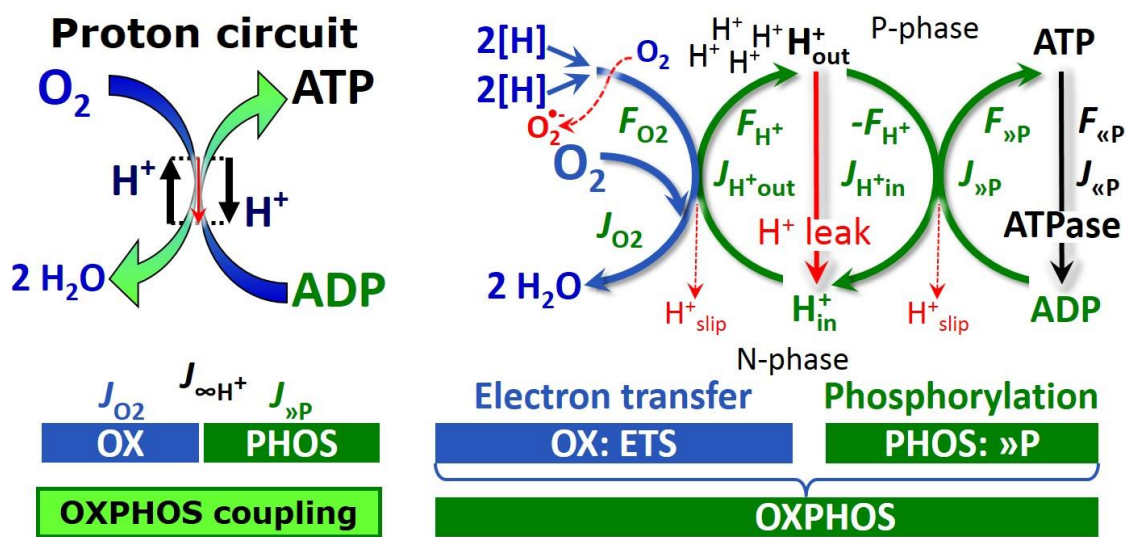


Fig. 2. The proton circuit and coupling in oxidative phosphorylation (OXPHOS). Oxygen flux, J_{O_2} , is coupled to the phosphorylation of ADP to ATP, $J_{\gg\text{P}}$, by the proton pumps of the electron transfer system, ETS, pushing the outward proton flux, $J_{\text{H}^+\text{out}}$, and generating the output protonmotive force, F_{H^+} . ATP synthase is driven by the input protonmotive force, $-F_{\text{H}^+}$, and inward proton flux, $J_{\text{H}^+\text{in}}$, to phosphorylate ADP to ATP. $2[\text{H}]$ indicates the reduced hydrogen equivalents of fuel substrates that provide the chemical input force, F_{O_2} [kJ/mol O_2], of the reaction with oxygen (molar Gibbs energy of reaction), typically in the range of -460 to -480 kJ/mol. The output force is given by the phosphorylation potential

difference (ADP phosphorylated to ATP), $F_{\gg P}$, which varies *in vivo* in a range of about 48 to 62 kJ/mol under physiological conditions. Proton turnover, $J_{\infty H^+}$, and ATP turnover, $J_{\infty P}$, proceed in the steady state at constant F_{H^+} , when $J_{\infty H^+} = J_{H^+out} = J_{H^+in}$, and at constant $F_{\gg P}$, when $J_{\infty P} = J_{\gg P} = J_{\ll P}$. $J_{\gg P}/J_{O_2}$ ($\gg P/O_2$) is two times the 'P/O' ratio of classical bioenergetics. The effective $\gg P/O_2$ ratio is diminished by: (1) the proton leak across the inner mitochondrial membrane from low pH in the P-phase to high pH in the N-phase (P, positive; N, negative); (2) cycling of other cations; (3) proton slip of the proton pumps when a proton effectively is not pumped; and (4) electron leak in the univalent reduction of oxygen (O_2 ; dioxygen) to superoxide anion radical ($O_2^{\cdot-}$). Modified from Gnaiger (2014).

Table 1. Coupling states and residual oxygen consumption in mitochondrial preparations in relation to respiration and phosphorylation rate, J_{O_2} and $J_{\gg P}$, and protonmotive force, F_{H^+} . Coupling states are established at kinetically saturating concentrations of fuel substrates and O_2 .

| State | J_{O_2} | $J_{\gg P}$ | F_{H^+} | Induced by: | Limited by: |
|--------|--|-------------|-----------|---|---|
| LEAK | L ; low proton leak-dependent respiration; | 0 | max. | (1) without ADP, L_N ; (2) max. ATP/ADP ratio, L_T (State 4); or (3) inhibition of the ADP phosphorylation system, L_{Omy} (State 4o) | $J_{\gg P}=0$; J_{O_2} by proton leak |
| OXPPOS | P ; high ADP-stimulated respiration | max. | high | Kinetically saturating [ADP] and $[P_i]$ (State 3, possibly without kinetic saturation of ADP) | $J_{\gg P}$ by phosphorylation system; or J_{O_2} by electron transfer system |
| ETS | E ; max. noncoupled respiration | 0 | low | Optimal external uncoupler concentration for maximum oxygen flux (State 3u) | J_{O_2} by electron transfer system |
| ROX | Rox ; min. residual O_2 consumption | 0 | 0 | Full inhibition of ETS or absence of substrates | J_{O_2} by non-ETS oxidation reactions |

OXPHOS state (Fig. 3): The respiratory state with kinetically saturating concentrations of O_2 , respiratory and phosphorylation substrates, and zero uncoupler, to provide an estimate of the maximal capacity of OXPHOS in any given pathway control state. Respiratory capacities at kinetically saturating substrate concentrations provide reference values or upper limits of performance, aiming at the generation of data sets for comparative purposes. Any effects of substrate kinetics are thus separated from reporting actual mitochondrial capacity for oxidation during coupled respiration, against which physiological activities can be evaluated.

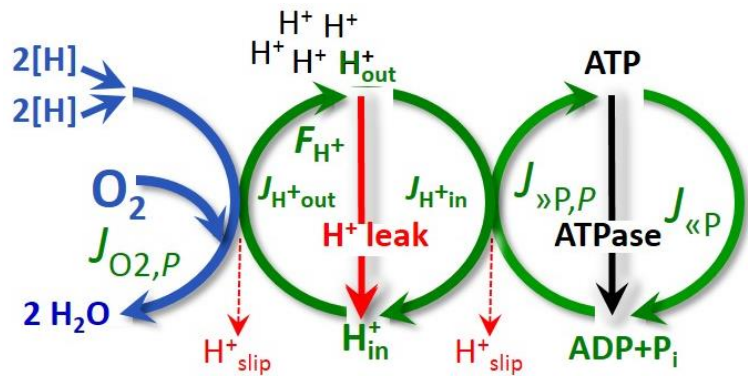


Fig. 3. OXPHOS state: Phosphorylation, $J_{\gg P}$, is stimulated by kinetically saturating [ADP] and inorganic phosphate, $[P_i]$, and is supported by a high protonmotive force, F_{H^+} . O_2 flux, $J_{O_2,P}$, is highly coupled at a maximum $\gg P/O_2$ ratio, $J_{\gg P,P}/J_{O_2,P}$ (See also Fig. 2).

As discussed previously, 0.2 mM ADP does not fully saturate flux in isolated mitochondria (Gnaiger 2001; Puchowicz *et al.* 2004); greater ADP concentration is required, particularly in permeabilized muscle fibres and cardiomyocytes, to overcome limitations by intracellular diffusion and by the reduced conductance of the outer mitochondrial membrane (Jepihhina *et al.* 2011, Illaste *et al.* 2012, Simson *et al.* 2016) either through interaction with tubulin (Rostovtseva *et al.* 2008) or other intracellular structures (Birkedal *et al.* 2014). In permeabilized muscle fibre bundles of high respiratory capacity, the apparent K_m for ADP increases up to 0.5 mM (Saks *et al.* 1998). This implies that >90% saturation is reached only at >5 mM ADP. Similar ADP concentrations are also required for accurate determination of OXPHOS capacity in human clinical cancer samples and permeabilized cells.

ETS state (Fig. 4): The ETS state is defined as the *noncoupled* state with kinetically saturating concentrations of O_2 , respiratory substrate and optimum *exogenous* uncoupler concentration for maximum O_2 flux, as an estimate of oxidative ETS capacity. Inhibition of respiration is observed at higher than optimum uncoupler

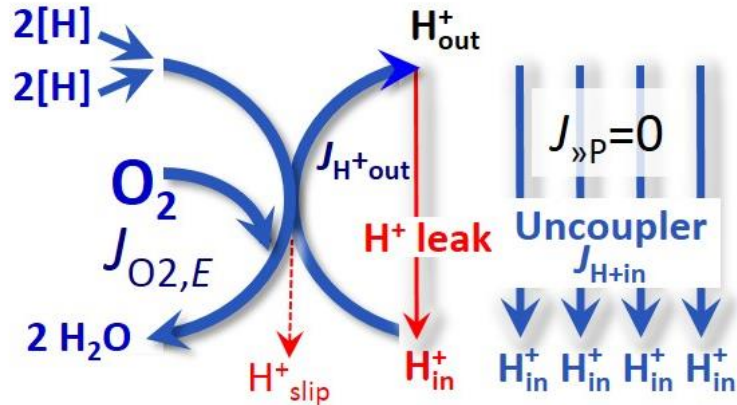


Fig. 4. ETS state: Noncoupled respiration, $J_{O_2,E}$, is maximum at optimum exogenous uncoupler concentration and phosphorylation is zero, $J_{\gg P}=0$ (See also Fig. 2).

concentrations. As a consequence of the nearly collapsed protonmotive force, the driving force is insufficient for phosphorylation and $J_{\gg P}=0$. The abbreviation State 3u is frequently used in bioenergetics, to indicate the state of maximum respiration without sufficient emphasis on the fundamental difference between OXPHOS capacity (*well coupled* with an *endogenous* uncoupled component) and ETS capacity (*noncoupled*).

LEAK state (Fig. 5): A state of mitochondrial respiration when O_2 flux mainly compensates for the proton leak in the absence of ATP synthesis, at kinetically saturating concentrations of O_2 and respiratory substrates. LEAK respiration is measured to obtain an indirect estimate of *in-*

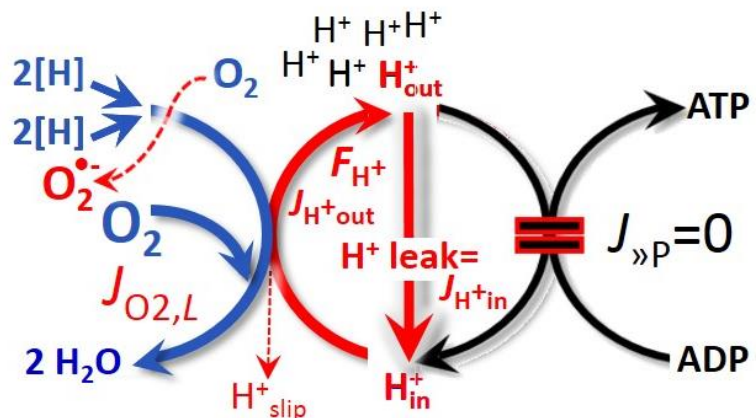


Fig. 5. LEAK state: Phosphorylation is arrested, $J_{\gg P}=0$, and oxygen flux, $J_{O_2,L}$, is controlled mainly by the proton leak, which equals J_{H^+in} , at maximum protonmotive force, F_{H^+} (See also Fig. 2).

trinsic uncoupling without addition of any experimental uncoupler: (1) in the absence of adenylates; (2) after depletion of ADP at maximum ATP/ADP ratio; or (3) after inhibition of the phosphorylation system by inhibitors of ATP synthase, such as oligomycin, or adenylate nucleotide translocase, such as carboxyatractyloside.

Proton leak: Proton leak is the *uncoupled* process in which protons are translocated across the inner mitochondrial membrane in the dissipative direction of the downhill protonmotive force without coupling to phosphorylation (**Fig. 5**). The proton leak flux depends on the protonmotive force, is a property of the inner mitochondrial membrane, and may be physiologically controlled. In particular, uncoupling mediated by uncoupling protein 1 (UCP1) is physiologically controlled, *e.g.*, in brown adipose tissue. UCP1 is a proton channel of the inner mitochondrial membrane facilitating the conductance of protons across the inner mitochondrial membrane. As consequence of this effective short-circuit, the protonmotive force diminishes, resulting in stimulation of electron transfer to oxygen and heat dissipation without phosphorylation of ADP. Mitochondrial injuries may lead to *dyscoupling* as a pathological or toxicological cause of *uncoupled* respiration, *e.g.*, as a consequence of opening the permeability transition pore. Dyscoupled respiration is distinguished from the experimentally induced *noncoupled* respiration in the ETS state. Under physiological conditions, the proton leak is the dominant contributor to the overall leak current.

Proton slip: Proton slip is the *decoupled* process in which protons are only partially translocated by a proton pump of the ETS and slip back to the original compartment (Dufour *et al.* 1996). Proton slip can also happen in association with the ATP-synthase, in which case the proton slips downhill across the membrane to the matrix without contributing to ATP synthesis. In each case, proton slip is a property of the proton pump and increases with the turnover rate of the pump.

Cation cycling: Proton leak is a leak current of protons. There can be other cation contributors to leak current including calcium and probably magnesium. Calcium current is balanced by Na/Ca exchange, which is balanced by Na/H exchange or K/H exchange. This is another effective uncoupling mechanism different from proton leak and slip.

Small differences of terms, *e.g.*, uncoupled, noncoupled, are easily overlooked and may be erroneously perceived as identical. Even with an attempt at rigorous definition, the common use of such terms may remain vague (**Table 2**).

Table 2. Distinction of terms related to coupling.

| Term | Respiration | »P/O ₂ | Note |
|-------------------------|-------------|-------------------|--|
| Fully coupled | $P - L$ | Max. | OXPPOS capacity corrected for LEAK respiration (Fig. 6) |
| Coupled | P | High | Phosphorylating respiration with a variable component of intrinsic LEAK respiration (Fig. 3) |
| Uncoupled, Decoupled | L | 0 | Nonphosphorylating respiration without added protonophore (Fig. 5) |
| Noncoupled | E | 0 | Nonphosphorylating respiration stimulated to maximum flux at optimum uncoupler concentration (Fig. 4) |
| Dyscoupled | P | Low | Pathologically increased uncoupling, mitochondrial dysfunction |

Besides the three fundamental coupling states of mitochondrial preparations, the following respiratory state also is relevant to assess respiratory function:

ROX: Residual oxygen consumption (ROX) is defined as O₂ consumption due to oxidative side reactions remaining after inhibition of the ETS. ROX is not a coupling state but represents a baseline that is used to correct mitochondrial respiration in defined coupling states. ROX is not necessarily equivalent to non-mitochondrial respiration, considering oxygen-consuming reactions in mitochondria not related to ETS, such as oxygen consumption in reactions catalyzed by monoamine oxidases (type A and B), monooxygenases (cytochrome P450 monooxygenases), dioxygenase (sulfur dioxygenase and trimethyllysine dioxygenase), several

hydroxylases, and more. The dependence of ROX-linked oxygen consumption needs to be studied in detail with respect to non-ETS enzyme activities, availability of specific substrates, oxygen concentration, and electron leakage leading to the formation of reactive oxygen species.

2.3. Classical terminology for isolated mitochondria

‘When a code is familiar enough, it ceases appearing like a code; one forgets that there is a decoding mechanism. The message is identical with its meaning’
(Hofstadter 1979).

Chance and Williams (1955; 1956) introduced five classical states of mitochondrial respiration and cytochrome redox states. **Table 3** shows a protocol with isolated mitochondria in a closed respirometric chamber, defining a sequence of respiratory states.

Table 3. Metabolic states of mitochondria (after Chance and Williams, 1956).

| State | [O ₂] | [ADP] | [Substrate] | Respiration rate | Rate-limiting substance |
|-------|-------------------|-------|-------------|------------------|-------------------------|
| 1 | >0 | Low | Low | Slow | ADP |
| 2 | >0 | High | ~0 | Slow | Substrate |
| 3 | >0 | High | High | Fast | Respiratory chain |
| 4 | >0 | Low | High | Slow | ADP |
| 5 | 0 | High | High | 0 | Oxygen |

State 1 is obtained after addition of isolated mitochondria to air-saturated isoosmotic/iso-tonic respiration medium containing inorganic phosphate, but no fuel substrates and no adenylates, *i.e.*, AMP, ADP, ATP.

State 2 is induced by addition of a high concentration of ADP (typically 100 to 300 μ M), which stimulates respiration transiently on the basis of endogenous fuel substrates and phosphorylates only a small portion of the added ADP. State 2 is then obtained at a low respiratory activity limited by zero endogenous fuel substrate availability (**Table 3**). If addition of specific inhibitors of respiratory complexes, such as rotenone, do not cause a further decline of oxygen

consumption, State 2 is equivalent to residual oxygen consumption (See below). If inhibition is observed, undefined endogenous fuel substrates are a confounding factor of pathway control by externally added substrates and inhibitors. In contrast to the original definition, an alternative protocol is frequently applied, in which State 2 is induced by addition of fuel substrate without ADP (LEAK state), followed by addition of ADP.

State 3 is the state stimulated by addition of fuel substrates while the ADP concentration is still high (**Table 3**) and supports coupled energy transformation through oxidative phosphorylation. 'High ADP' is a concentration of ADP specifically selected to allow the measurement of State 3 to State 4 transitions of isolated mitochondria in a closed respirometric system. Repeated ADP titration re-establishes State 3 at 'high ADP'. Starting at oxygen concentrations near air-saturation (ca. 200 μM O_2 at sea level and 37 $^\circ\text{C}$), the total ADP concentration added must be low enough (typically 100 to 300 μM) to allow phosphorylation to ATP at a coupled oxygen consumption that does not lead to oxygen depletion during the transition to State 4. In contrast, kinetically saturating ADP concentrations usually are an order of magnitude higher than 'high ADP', *e.g.* 2.5 mM in isolated mitochondria.

State 4 is reached only if the mitochondrial preparation is intact and well-coupled. Depletion of ADP by phosphorylation to ATP leads to a decline in oxygen consumption in the transition from State 3 to State 4. Under these conditions, a maximum protonmotive force and high ATP/ADP ratio are maintained, and the $\gg\text{P}/\text{O}_2$ ratio can be calculated. State 4 respiration reflects intrinsic proton leak and contaminating ATP hydrolysis activity. Oxygen consumption in State 4 is an overestimation of LEAK respiration if the intrinsic ATP hydrolysis activity recycles some ATP to ADP, $J_{\ll\text{P}}$, which stimulates respiration coupled to phosphorylation, $J_{\gg\text{P}} > 0$. This can be tested by inhibition of the phosphorylation system using oligomycin, ensuring that $J_{\gg\text{P}} = 0$ (State 4o). Alternatively, sequential ADP titrations re-establish State 3, followed by State 3 to State 4 transitions while sufficient oxygen is available. However, anoxia may be reached before exhaustion of ADP (State 5).

State 5 is the state after exhaustion of oxygen in a closed respirometric chamber. Diffusion of oxygen from the surroundings into the aqueous solution may be a confounding factor preventing complete anoxia (Gnaiger 2001).

2.4. Coupling states and respiratory rates

It is important to distinguish metabolic systems or modules from metabolic states and the corresponding metabolic rates; for example: electron transfer system, ETS (**Fig. 6**), ETS state, and ETS capacity, E , respectively (**Table 1**). The protonmotive force is *high* in the OXPHOS state when it drives phosphorylation, *maximum* in the LEAK state of coupled mitochondria, driven by LEAK respiration at a minimum back flux of protons to the matrix side, and *very low* in the ETS state when uncouplers short-circuit the proton cycle (**Table 1**).

The three coupling states, ETS, LEAK and OXPHOS, are presented in a schematic context with the corresponding respiratory rates, abbreviated as E , L and P , respectively. This clarifies that E may exceed or be equal to P , but E cannot theoretically be lower than P . $E < P$ must be discounted as an artefact, which may be caused experimentally by: (1) using too low uncoupler concentrations; (2) using high uncoupler concentrations which inhibit the ETS (Gnaiger 2008); (3) high oligomycin concentrations applied for measurement of L before titrations of uncoupler, when oligomycin exerts an inhibitory effect on E ; or (4) loss of oxidative capacity during the time course of the respirometric assay, since E is measured subsequently to P . On the other hand, the excess ETS capacity is overestimated if non-saturating $[P_i]$ or $[ADP]$ (State 3) are used.

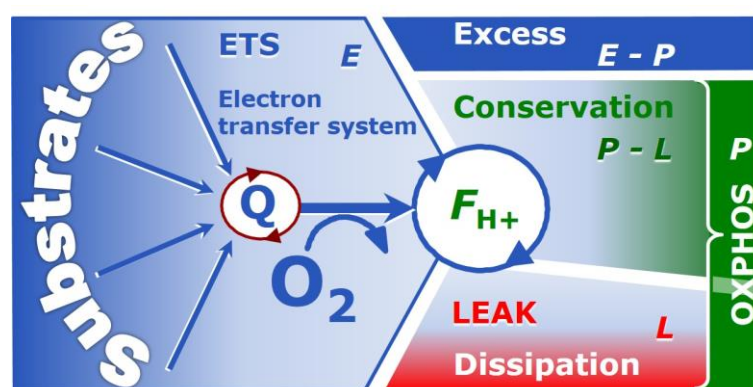
$E > P$ is observed in many types of mitochondria and depends on: (1) the excess ETS capacity pushing the phosphorylation system (**Fig. 1B**) to the limit of its *capacity of utilizing* the protonmotive force; (2) the pathway control state with single or multiple electron input into the Q-junction and involvement of three or fewer coupling sites determining the H^+_{out}/O_2 *coupling stoichiometry* (**Fig. 1A**); (3) the *biochemical coupling efficiency* expressed as $(E-L)/E$, since an

increase of L causes P to increase towards the limit of E . The *excess* $E-P$ capacity, $E-P$, therefore, provides a sensitive diagnostic indicator of specific injuries of the phosphorylation system, under conditions when E remains constant but P declines relative to controls (**Fig. 6**). Substrate cocktails supporting simultaneous convergent electron transfer to the Q-junction for reconstitution of TCA cycle function establish pathway control states with high ETS capacity, and consequently increase the sensitivity of the $E-P$ assay.

When subtracting L from P , the dissipative LEAK component in the OXPHOS state may be overestimated. This can be avoided by measurement of LEAK respiration in a state when the protonmotive force is titrated, *e.g.*, by an ETS inhibitor, to the slightly lower value maintained in the OXPHOS state. Any turnover-dependent components of proton leak and slip, however, are underestimated under these conditions (Garlid *et al.* 1993). In general, it is inappropriate to use the term *ATP production* for the difference of oxygen consumption measured in states P and L . The difference $P-L$ is the upper limit of the part of OXPHOS capacity that is freely available for ATP production (corrected for LEAK respiration) and is fully coupled to phosphorylation with a maximum mechanistic stoichiometry (**Fig. 6**).

Fig. 6. Four-compartmental model of oxidative phosphorylation.

Respiratory states (ETS, OXPHOS, LEAK) and corresponding rates (E , P , L) are connected by the protonmotive force, F_{H^+} . Electron transfer system capacity, E , is partitioned



into the dissipative LEAK respiration, L , partial conservation of the protonmotive exergy as the phosphorylation exergy in net OXPHOS capacity, $P-L$, and the excess capacity, $E-P$. Modified from Gnaiger (2014).

3. States and rates

3.1. The steady-state

Mitochondria represent a thermodynamically open system functioning as a biochemical transformation system in non-equilibrium states. State variables (protonmotive force; redox states) and metabolic fluxes (*rates*) are measured in defined mitochondrial respiratory *states*. Strictly, steady states can be obtained only in open systems, in which changes due to *internal* transformations, *e.g.*, O₂ consumption, are instantaneously compensated for by *external* flows *e.g.*, O₂ supply, such that oxygen concentration does not change in the system (Gnaiger 1993b). Mitochondrial respiratory states monitored in closed systems satisfy the criteria of pseudo-steady states for limited periods of time, when changes in the system (concentrations of O₂, fuel substrates, ADP, P_i, H⁺) do not exert significant effects on metabolic fluxes (respiration, phosphorylation). Such pseudo-steady states require buffers and kinetically saturating concentrations of substrates to be maintained, and thus depend on the kinetics of the processes under investigation.

Flux per chamber volume, J_V : The volume-specific *flux of a chemical reaction* r is the time derivative of the advancement of the reaction per unit volume, $d_r \xi_B / dt \cdot V^{-1}$ [(mol·s⁻¹)·L⁻¹]. The *rate of concentration change* is dc_B / dt [(mol·L⁻¹)·s⁻¹], where concentration is $c_B = n_B / V$. It is helpful to make the subtle distinction between [mol·s⁻¹·L⁻¹] and [mol·L⁻¹·s⁻¹] for the fundamentally different quantities volume-specific flux and rate of concentration change, which merge to a single concept only in closed systems. In open systems, external flows (such as O₂ supply) are distinguished from internal transformations (metabolic flow, O₂ consumption). In a closed system, external flows of all substances are zero and O₂ consumption (internal flow), I_{O_2} [pmol·s⁻¹], causes a decline of the amount of O₂ in the system, n_{O_2} [nmol]. Normalization of these quantities for the volume of the system, V [L=dm³], yields volume-specific O₂ flux, $J_{V,O_2} = I_{O_2} / V$ [nmol·s⁻¹·L⁻¹], and O₂ concentration, $[O_2]$ or $c_{O_2} = n_{O_2} / V$ [nmol·mL⁻¹=μmol·L⁻¹=μM]. Instrumental background O₂ flux is due to external flux into a non-

ideal closed respirometer, such that total volume-specific flux has to be corrected for instrumental background O₂ flux. J_{V,O_2} is relevant mainly for methodological reasons and should be compared with the accuracy of instrumental resolution of background-corrected flux, *e.g.* ± 1 nmol·s⁻¹·L⁻¹ (Gnaiger 2001). ‘Metabolic’ indicates O₂ flux corrected for instrumental background O₂ flux and chemical background O₂ flux due to autoxidation of chemical components added to the incubation medium.

3.2. The protonmotive force and proton flow

Table 4. Protonmotive force and flow matrix. Rows: Electrical and chemical isomorphous format (*e* and *n*). The Faraday constant, F , converts protonmotive force and flow from *isomorphous format e* to *n*. Columns: The protonmotive force is the sum of *partial isomorphous forces* F_{el} and F_{d,H^+} . In contrast to force (state), the conjugated flow (rate) cannot be partitioned.

| State | Force | electric | + | chemical | Unit | Notes | |
|----------------------------------|--------------------------------|-------------------------|---|----------------------|-------|------------------|----------------------|
| Protonmotive force, <i>e</i> | Δp_{H^+} | = $\Delta \Psi$ | + | $\Delta \mu_{H^+}/F$ | J/C | Eq. 1 <i>e</i> | |
| Chemiosmotic potential, <i>n</i> | $\Delta \tilde{\mu}_{H^+}$ | = $\Delta \Psi \cdot F$ | + | $\Delta \mu_{H^+}$ | J/mol | Eq. 1 <i>n</i> | |
| State | Isomorph <i>e</i> and <i>n</i> | Force, $F_{H^+/i}$ | = | el | + | d,H ⁺ | |
| | Electric charge, <i>e</i> | $F_{H^+/e}$ | = | $F_{el/e}$ | + | $F_{d,H^+/e}$ | J/C Eq. 2 <i>e</i> |
| | Amount of substance, <i>n</i> | $F_{H^+/n}$ | = | $F_{el/n}$ | + | $F_{d,H^+/n}$ | J/mol Eq. 2 <i>n</i> |
| Rate | Isomorph <i>e</i> and <i>n</i> | Flow, $I_{H^+/i}$ | = | <i>e</i> | or | <i>n</i> | |
| | Electric charge, <i>e</i> | $I_{H^+/e}$ | | $I_{H^+/e}$ | | | C/s |
| | Amount of substance, <i>n</i> | $I_{H^+/n}$ | | | | $I_{H^+/n}$ | mol/s |

Eq. 1: The Faraday constant, F , is the product of elementary charge ($e=1.602177 \cdot 10^{-19}$ ·C) and the Avogadro (Loschmidt) constant ($N_A=6.022136 \cdot 10^{23}$ ·mol⁻¹), $F=eN_A=96,485.3$ C/mol. $\Delta \tilde{\mu}_{H^+}$ is the chemiosmotic potential difference. Eqs. 1*e* and 1*n* are the classical representations of Eqs. 2*e* and 2*n*.

Eq. 2: The protonmotive force is F_{H^+} , expressed either in isomorphous format *e* or *n*. $F_{el/e} \equiv \Delta \Psi$ is the partial protonmotive force (el) acting generally on charged motive molecules (*i.e.* ions that are

displaceable across the inner mitochondrial membrane). In contrast, $F_{d,H^+/n} \equiv \Delta\mu_{H^+}$ is the partial protonmotive force specific for proton displacement (d,H^+). The sign of the force is positive for endergonic, negative for exergonic transformations. The sign of the flow depends on the definition of the compartmental direction of the translocation (**Fig. 2**). Flow \times force = $I_{H^+/e} \cdot F_{H^+/e} = I_{H^+/n} \cdot F_{H^+/n} = \text{Power [J/s=W]}$.

The protonmotive force across the inner mitochondrial membrane (Mitchell and Moyle 1967) was introduced most beautifully in the *Grey Book 1966* (see Mitchell 2011),

$$\Delta p_{H^+} = \Delta\psi + \Delta\mu_{H^+}/F \quad (\text{Eq. 1})$$

The protonmotive force consists of two partial forces: (1) The electrical part, $\Delta\psi$, is the difference of charge (electric potential difference) and is not specific for H^+ . (2) The chemical part, $\Delta\mu_{H^+}$, is the chemical potential difference in H^+ , is proportional to the pH difference, and incorporates the Faraday constant (**Table 4**).

Faraday constant, $F = eN_A$ [C/mol] (**Table 4**), enables the conversion between protonmotive force, $F_{H^+/e} \equiv \Delta p_{H^+}$ [J/C], expressed per *motive charge*, e [C], and protonmotive force or electrochemical potential difference, $F_{H^+/n} \equiv \Delta\tilde{\mu}_{H^+} = \Delta p_{H^+} \cdot F$ [J/mol], expressed per *motive amount of protons*, n [mol]. Proton charge, e , and amount of substance, n , define the units for the isomorphic formats. Taken together, F converts protonmotive force and flow from isomorphic format e to n (Eq. 3; see also **Table 4**, Eq. 2),

$$F_{H^+/n} = F_{H^+/e} \cdot eN_A \quad (\text{Eq. 3.1})$$

$$I_{H^+/n} = I_{H^+/e} / (eN_A) \quad (\text{Eq. 3.2})$$

In each format, the protonmotive force is expressed as the sum of two partial forces. The concept expressed by the complex symbols in Eq. 1 can be explained and visualized more easily by *partial isomorphic forces* as the components of the protonmotive force:

Electrical part of the protonmotive force: (1) Isomorph e : $F_{el/e} \equiv \Delta\psi$ is the electrical part of the protonmotive force expressed in units joule per coulomb, *i.e.* volt [V=J/C]. $F_{el/e}$ is

defined as partial Gibbs energy change per *motive elementary charge*, e [C], not specific for proton charge (**Table 4**, Eq. 2e). (2) Isomorph n : $F_{el/n} \equiv \Delta\Psi \cdot F$ is the electric force expressed in units joule per mole [J/mol], defined as partial Gibbs energy change per *motive amount of charge*, n [mol], not specific for proton charge (**Table 4**, Eq. 2n).

Chemical part of the protonmotive force: (1) Isomorph n : $F_{d,H+/n} \equiv \Delta\mu_{H^+}$ is the chemical part (diffusion, displacement of H^+) of the protonmotive force expressed in units joule per mole [J/mol]. $F_{d,H+/n}$ is defined as partial Gibbs energy change per *motive amount of protons*, n [mol] (**Table 4**, Eq. 2n). (2) Isomorph e : $F_{d,H+/e} \equiv \Delta\mu_{H^+}/F$ is the chemical force expressed in units joule per coulomb [V], defined as partial Gibbs energy change per *motive amount of protons expressed in units of electric charge*, e [C], but specific for proton charge (**Table 4**, Eq. 2e).

Protonmotive means that protons can be moved across the mitochondrial membrane. Force is a measure of the potential for motion. Motion is relative and not absolute (Principle of Galilean Relativity); likewise there is no absolute potential, but (isomorphic) forces are potential differences (equations in **Table 5**). An electric partial force expressed in the format of electric charge, $F_{el/e}$, of -0.2 V (Eq. 8e) is equivalent to force in the format of amount, $F_{el,H+/n}$, of 19 $\text{kJ}\cdot\text{mol}^{-1} H^+_{\text{out}}$ (Eq. 8n). For a ΔpH of 1 unit, the chemical partial force in the format of amount, $F_{d,H+/n}$, changes by 6 $\text{kJ}\cdot\text{mol}^{-1}$ (Eq. 9n) and chemical force in the format of charge $F_{d,H+/e}$ changes by 0.06 V (**Table 5**, Eq. 9e). Considering a driving force of -470 $\text{kJ}\cdot\text{mol}^{-1} O_2$ for oxidation, the thermodynamic limit of the H^+_{out}/O_2 ratio is reached at a value of $470/19=24$, compared to a mechanistic stoichiometry of 20 (**Fig. 1**).

Table 5. Power, exergy, force, flow, and advancement.

| Expression | Symbol | Definition | Unit | Notes |
|-------------------|----------------------|--|---------------------------------------|--------|
| Power | P_{tr} | $P_{tr} = I_{tr} \cdot F_{tr} = \partial_{tr}G \cdot \partial t$ | $\text{W}=\text{J}\cdot\text{s}^{-1}$ | Eq. 4 |
| Force, isomorphic | F_{tr} | $F_{tr} = \partial G \cdot \partial_{tr}\zeta^{-1}$ | $\text{J}\cdot\text{X}^{-1}$ | Eq. 5 |
| Flow, isomorphic | I_{tr} | $I_{tr} = d_{tr}\zeta \cdot dt^{-1}$ | $\text{X}\cdot\text{s}^{-1}$ | Eq. 6 |
| Advancement, n | $d_{tr}\zeta_{H+/n}$ | $d_{tr}\zeta_{H+/n} = dn_{H^+} \cdot \nu_{H^+}^{-1}$ | mol | Eq. 7n |
| Advancement, e | $d_{tr}\zeta_{H+/e}$ | $d_{tr}\zeta_{H+/e} = de_{H^+} \cdot \nu_{H^+}^{-1}$ | C | Eq. 7e |

| | | | | |
|---|--------------|--|---|--------|
| Electric partial force, e | $F_{el/e}$ | $F_{el/e} \equiv \Delta\Psi$ | V | Eq. 8e |
| Electric partial force, n | $F_{el/n}$ | $\Delta\Psi \cdot F = 96.5 \cdot \Delta\text{pH}$ | $\text{kJ} \cdot \text{mol}^{-1}$ | Eq. 8n |
| Chemical partial force, e at 37 °C | $F_{d,H+/e}$ | $\Delta\mu_{H^+}/F = -\ln(10) \cdot RT/F \cdot \Delta\text{pH}$ $= -0.06 \cdot \Delta\text{pH}$ | V $\text{J} \cdot \text{C}^{-1}$ | Eq. 9e |
| Chemical partial force, n at 37 °C | $F_{d,H+/n}$ | $\Delta\mu_{H^+} = -\ln(10) \cdot RT \cdot \Delta\text{pH}$ $= -5.9 \cdot \Delta\text{pH}$ | $\text{J} \cdot \text{mol}^{-1}$ $\text{kJ} \cdot \text{mol}^{-1}$ | Eq. 9n |

Eq. 4 to 7: An isomorphic motive entity or transformant, expressed in unit X, is defined for any transformation, tr. $X=\text{mol}$ or C in proton translocation. For comparison, in a mechanical, vectorial advancement, $d_{\text{me}}\xi$ [m], the unit of the *force* is newton, F_{me} [$\text{N}=\text{J} \cdot \text{m}^{-1}$], and *flow* is the velocity, $v=d_{\text{me}}\xi/dt$ [$\text{m} \cdot \text{s}^{-1}$], such that the flow-force product yields mechanical power, P_{me} [W] (Cohen *et al.* 2008). The corresponding *vectorial flux* (flow density per area) is velocity per cross-sectional area [$\text{s}^{-1} \cdot \text{m}^{-1}$]. The *scalar flux* lacks spatial information in a given volume, such that flux ($\text{m} \cdot \text{s}^{-1}$ per volume [$\text{s}^{-1} \cdot \text{m}^{-2}$]) times force yields volume-specific power, P_{vme} [$\text{W} \cdot \text{m}^{-3}$].

Eq. 5: $\partial_{\text{tr}}G$ [J] is the partial Gibbs energy change (exergy) in the advancement of transformation tr.

Eq. 6: For $X=\text{C}$, flow is electric current, I_{el} [$\text{A} = \text{C} \cdot \text{s}^{-1}$].

Eq. 7n: For a chemical reaction, the advancement of reaction r is $d_r\xi_B=d_rn_B \cdot v_B^{-1}$ [mol]. The stoichiometric number is $v_B=-1$ or $v_B=1$, depending on B being a product or substrate, respectively, in reaction r involving one mole of B. The conjugated *intensive* molar quantity, $F_{r,B} = \partial G/\partial_r\xi_B$ [$\text{J} \cdot \text{mol}^{-1}$], is the chemical force of reaction or *reaction-motive* force per stoichiometric amount of B. In reaction kinetics, d_rn_B is expressed as a volume-specific quantity, which is the partial contribution to the total concentration change of B, $d_r c_B=d_r n_B/V$ and $d c_B=d n_B/V$, respectively. In open systems with constant volume V , $d c_B=d_r c_B+d_e c_B$, where r indicates the *internal* reaction and e indicates the *external* flux of B into the unit volume of the system. At steady state the concentration does not change, $d c_B=0$, when $d_r c_B$ is compensated for by the external flux of B, $d_r c_B=-d_e c_B$ (Gnaiger 1993b). Alternatively, $d c_B=0$ when B is held constant by different coupled reactions in which B acts as a substrate or a product.

Eq. 8e: Scalar potential difference across the mitochondrial membrane. In a scalar electric transformation (flux of charge, *i.e.* current, from the matrix space to the intermembrane and

extramitochondrial space) the motive force is the difference of charge. The endergonic direction of translocation is defined in **Fig. 2** as $H^+_{in} \rightarrow H^+_{out}$.

Eq. 8n: $F=96.5 \text{ (kJ}\cdot\text{mol}^{-1})/V$.

Eq. 9: Note that the electric partial force is independent of temperature (Eq. 8), but the chemical partial force depends on absolute temperature, T [K].

Eq. 9e: RT is the gas constant times absolute temperature. $\ln(10)\cdot RT/F = 59.16$ and 61.54 mV at 298.15 and 310.15 K (25 and 37 °C), respectively.

Eq. 9n: $\ln(10)\cdot RT = 5.708$ and $5.938 \text{ kJ}\cdot\text{mol}^{-1}$ at 298.15 and 310.15 K (25 and 37 °C), respectively.

3.3. Forces and flows in physics and irreversible thermodynamics

According to its definition in physics, a potential difference and as such the *protonmotive force*, Δp_{H^+} , is not a force *per se* (Cohen *et al.* 2008). The fundamental forces of physics are distinguished from *motive forces* of statistical and irreversible thermodynamics. Complementary to the attempt towards unification of fundamental forces defined in physics, the concepts of Nobel laureates Lars Onsager, Erwin Schrödinger, Ilya Prigogine and Peter Mitchell (even if expressed in apparently unrelated terms) unite the diversity of *generalized* or ‘isomorphic’ *flow-force* relationships, the product of which links to the dissipation function and Second Law of thermodynamics (Schrödinger 1944; Prigogine 1967). A *motive force* is the derivative of potentially available or ‘free’ energy (exergy) per isomorphic *motive* unit (force=exergy/motive unit; in integral form, this definition takes care of non-isothermal processes). In the framework of flow-force relationships, a potential difference is an isomorphic force, F_{tr} , involved in an exergy transformation, defined as the *partial* derivative of Gibbs energy per advancement of the transformation (**Table 5**, Eq. 5). This formal generalization represents an appreciation of the conceptual beauty of Peter Mitchell’s innovation of the protonmotive force against the background of the established paradigm of the electromotive force (emf) defined at the limit of zero current (Cohen *et al.* 2008). Perhaps the first account of a *motive force* in energy transformation

can be traced back to the Peripatetic school around 300 BC in the context of moving a lever, up to Newton's motive force proportional to the alteration of motion (Coopersmith 2010).

Vectorial and scalar forces, and fluxes: In chemical reactions and osmotic or diffusion processes occurring in a closed heterogeneous system, such as a chamber containing isolated mitochondria, scalar transformations occur without measured spatial direction but between separate compartments (translocation between the matrix and intermembrane space) or between energetically-separated chemical substances (reactions from substrates to products). Hence, the corresponding fluxes are not vectorial but scalar, and are expressed per volume and not per membrane area. The corresponding motive forces are also scalar potential *differences* across the membrane (**Table 5**), without taking into account the *gradients* across the 6 nm thick inner mitochondrial membrane (Rich 2003).

3.4. Coupling, efficiency, and power

Coupling: In energetics (ergodynamics), coupling is defined as an exergy transformation fuelled by an exergonic (downhill) input process driving the advancement of an endergonic (uphill) output process. The (negative) output/input power ratio is the efficiency of a coupled energy transformation. Power is closely linked to the dissipation function (Prigogine 1967) and is the product of flow times isomorphic force (**Table 5**, Eq. 4; Gnaiger 1993b). At the limit of maximum efficiency of a completely coupled system, the (negative) input power equals the (positive) output power, such that the total power approaches zero at the maximum efficiency of 1.

Loss of coupling by uncoupling, decoupling, and dyscoupling lowers the efficiency. Such uncoupling is different from switching to mitochondrial pathways that involve fewer than three coupling sites (Complexes CI, CIII and CIV), bypassing CI through multiple electron entries into the Q-junction (**Fig. 1**). A bypass of CIV is provided by alternative oxidases, which reduce

oxygen without proton translocation. Reprogramming mitochondrial pathways may be considered as a switch of gears (stoichiometry) rather than uncoupling (loosening the stoichiometry).

Coupled versus bound processes: Since the chemiosmotic theory describes the mechanism of coupling in OXPHOS, it may be interesting to ask if the electrical and chemical parts of proton translocation are coupled processes. This is not the case according to the definition of coupling. If the coupling mechanism is disengaged, the output process becomes independent of the input process, and both proceed in their downhill (exergonic) direction (**Fig. 2**). It is not possible to physically uncouple the electrical and chemical processes, which are only *theoretically* partitioned as electrical and chemical components and can be measured separately. If partial processes are non-separable, *i.e.*, cannot be uncoupled, then these are not *coupled* but are defined as *bound* processes. The electrical and chemical parts are tightly bound partial forces of the protonmotive force, since the flow cannot be partitioned but expressed only in either an electrical or chemical isomorphic format (**Table 4**).

4. Normalization: flows and fluxes

4.1. Extensive expressions and size-specific normalization

Application of common and generally defined units is required for direct transfer of reported results into a database. The second [s] is the *SI* unit for the base quantity *time*. It is also the standard time-unit used in solution chemical kinetics. **Table 6** lists some conversion factors to obtain *SI* units. The term *rate* is too general and not useful for a database (**Fig. 7**). The inconsistency of the meanings of rate becomes fully apparent when considering Galileo Galilei's famous principle, that 'bodies of different weight all fall at the same rate (have a constant acceleration)' (Coopersmith 2010).

Extensive quantities: An extensive quantity increases proportionally with system size. The magnitude of an extensive quantity is completely additive for non-interacting subsystems,

such as mass or flow expressed per defined system. The magnitude of these quantities depends on the extent or size of the system (Cohen *et al.* 2008).

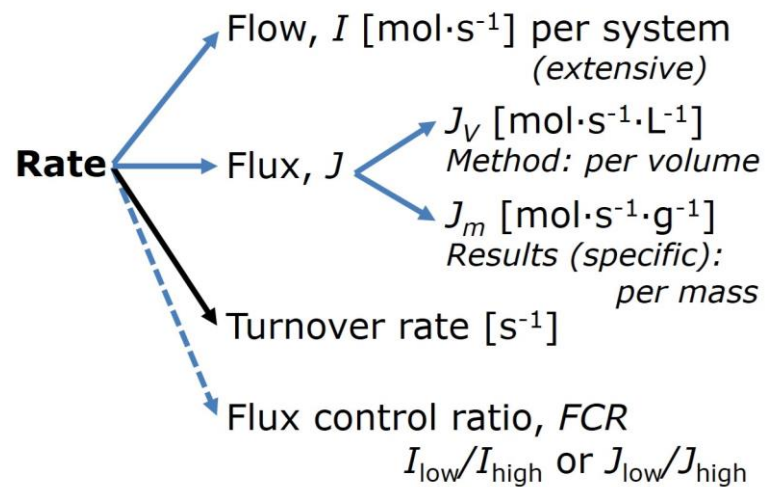
Size-specific quantities: ‘The adjective *specific* before the name of an extensive quantity is often used to mean *divided by mass*’ (Cohen *et al.* 2008). Mass-specific flux is flow divided by mass of the system. A mass-specific quantity is independent of the extent of non-interacting homogenous subsystems. Tissue-specific quantities are of fundamental interest in comparative mitochondrial physiology, where *specific* refers to the *type* rather than *mass* of the tissue. The term *specific*, therefore, must be further clarified, such that tissue mass-specific, *e.g.*, muscle mass-specific quantities are defined.

Molar quantities: ‘The adjective *molar* before the name of an extensive quantity generally means *divided by amount of substance*’ (Cohen *et al.* 2008). The notion that all molar quantities then become *intensive* causes ambiguity in the meaning of *molar Gibbs energy*. It is important to emphasize the fundamental difference between normalization for amount of substance *in a system* or for amount of motive substance *in a transformation*. When the Gibbs energy of a system, G [J], is divided by the amount of substance B in the system, n_B [mol], a *size-specific* molar quantity is obtained, $G_B = G/n_B$ [J·mol⁻¹], which is not any force at all. In contrast, when the partial Gibbs energy change, $\partial_r G$ [J], is divided by the motive amount of substance B in reaction r (advancement of reaction), $\partial_r \xi_B$ [mol], the resulting intensive molar quantity, $F_{r,B} = \partial G / \partial_r \xi_B$ [J·mol⁻¹], is the chemical motive force of reaction r involving 1 mol B (Table 5, Note to Eq. 7).

Flow per system, I : In analogy to electrical terms, flow as an extensive quantity (I ; per system) is distinguished from flux as a size-specific quantity (J ; per system size) (Fig. 7). Electric current is flow, I_{el} [A = C·s⁻¹] per system (extensive quantity). When dividing this extensive quantity by system size (membrane area), a size-specific quantity is obtained, which is electric flux (electric current density), J_{el} [A·m⁻² = C·s⁻¹·m⁻²].

Fig. 7. Different meanings of rate may lead to confusion, if the normalization is not sufficiently specified. Results are frequently expressed as mass-specific flux, J_m , per mg protein, dry or wet weight (mass). Cell volume, V_{cell} , or mitochondrial volume, V_{mt} , may be used for normalization (volume-specific

flux, $J_{V_{\text{cell}}}$ or $J_{V_{\text{mt}}}$), which then must be clearly distinguished from flux, J_V , expressed for methodological reasons per volume of the measurement system, or flow per cell, I_X .



Size-specific flux, J : Metabolic O_2 flow per tissue increases as tissue mass is increased. Tissue mass-specific O_2 flux should be independent of the size of the tissue sample studied in the instrument chamber, but volume-specific O_2 flux (per volume of the instrument chamber, V) should increase in direct proportion to the amount of sample in the chamber. Accurate definition of the experimental system is decisive: whether the experimental chamber is the closed, open, isothermal or non-isothermal *system* with defined volume as part of the measurement apparatus, in contrast to the experimental *sample* in the chamber (**Table 6**). Volume-specific O_2 flux depends on mass-concentration of the sample in the chamber, but should be independent of the chamber volume. There are practical limitations to increasing the mass-concentration of the sample in the chamber, when one is concerned about crowding effects and instrumental time resolution.

Sample concentration C_{mX} : Normalization for sample concentration is required for reporting respiratory data. Consider a tissue or cells as the sample, X , and the sample mass, m_X [g] from which a mitochondrial preparation is obtained. The sample mass is frequently measured as wet or dry weight ($m_X \equiv W_w$ or W_d [g]), or as amount of tissue or cell protein ($m_X \equiv m_{\text{Protein}}$).

In the case of permeabilized tissues, cells, and homogenates, the sample concentration, $C_{mX}=m_X/V$ [$\text{g}\cdot\text{L}^{-1}$], is simply the mass of the subsample of tissue that is transferred into the instrument chamber. Part of the mitochondria from the tissue is lost during preparation of isolated mitochondria, and only a fraction of mitochondria is obtained, expressed as the mitochondrial yield (**Fig. 8**). At a high mitochondrial yield the sample of isolated mitochondria is more representative of the total mitochondrial population than when the yield is low. Determination of the mitochondrial yield is based on measurement of the concentration of a mitochondrial marker in the tissue homogenate, $C_{\text{mte,thom}}$, which simultaneously provides information on the specific mitochondrial density in the sample (**Fig. 8**).

Mass-specific flux, J_{mX,O_2} : Mass-specific flux is obtained by expressing respiration per mass of sample, m_X [g]. X is the type of sample, *e.g.*, tissue homogenate, permeabilized fibres or cells. Volume-specific flux is divided by mass concentration of X , $J_{mX,O_2} = J_{V,O_2}/C_{mX}$; or flow per cell is divided by mass per cell, $J_{m\text{cell},O_2} = I_{\text{cell},O_2}/M_{\text{cell}}$. If mass-specific O_2 flux is constant and independent of sample size (expressed as mass), then there is no interaction between the subsystems. A 1.5 mg and a 3.0 mg muscle sample respire at identical mass-specific flux. Mass-specific O_2 flux, however, may change with the mass of a tissue sample, cells or isolated mitochondria in the measuring chamber, in which case the nature of the interaction becomes an issue.

Number concentration, C_{NX} : The experimental *number concentration* of sample in the case of cells or animals, *e.g.*, nematodes is $C_{NX}=N_X/V$ [$X\cdot\text{L}^{-1}$], where N_X is the number of cells or animals in the chamber (**Table 6**).

Flow per sample entity, I_{X,O_2} : A special case of normalization is encountered in respiratory studies with permeabilized (or intact) cells. If respiration is expressed per cell, the O_2 flow per measurement system is replaced by the O_2 flow per cell, I_{cell,O_2} (**Table 6**). O_2 flow can be calculated from volume-specific O_2 flux, J_{V,O_2} [$\text{nmol}\cdot\text{s}^{-1}\cdot\text{L}^{-1}$] (per V of the measurement chamber [L]), divided by the number concentration of cells, $C_{N_{\text{ce}}}=N_{\text{ce}}/V$ [$\text{cell}\cdot\text{L}^{-1}$], where N_{ce} is the

number of cells in the chamber. Cellular O₂ flow can be compared between cells of identical size. To take into account changes and differences in cell size, further normalization is required to obtain cell size-specific or mitochondrial marker-specific O₂ flux (Renner *et al.* 2003).

The complexity changes when the sample is a whole organism studied as an experimental model. The well-established scaling law in respiratory physiology reveals a strong interaction of O₂ consumption and individual body mass of an organism, since *basal* metabolic rate (flow) does not increase linearly with body mass, whereas *maximum* mass-specific O₂ flux, $\dot{V}_{O_{2max}}$, or $\dot{V}_{O_{2maxpeak}}$, is approximately constant across a large range of individual body mass (Weibel and Hoppeler 2005), with individuals, breeds, and certain species deviating substantially from this general relationship. $\dot{V}_{O_{2maxpeak}}$ of human endurance athletes is 60 to 80 mL O₂·min⁻¹·kg⁻¹ body mass, converted to $J_{m,O_{2peak}}$ of 45 to 60 nmol·s⁻¹·g⁻¹ (**Table 8**).

4.2. Normalization for mitochondrial content

Mitochondrial concentration, C_{mte} , and mitochondrial markers: Mitochondrial organelles comprise a cellular reticulum that is in a continual flux of fusion and fission. Hence the definition of an "amount" of mitochondria is often misconceived: mitochondria cannot be counted as a number of occurring elements. Therefore, quantification of the "amount" of mitochondria depends on measurement of a chosen mitochondrial markers. 'Mitochondria are the structural and functional elemental units of cell respiration' (Gnaiger 2014). The quantity of a mitochondrial marker can be considered as the measurement of the amount of *elemental mitochondrial units* or *mitochondrial elements*, mte. However, since mitochondrial quality changes under certain stimuli, particularly in mitochondrial dysfunction, some markers can vary while other markers are unchanged. (1) Structural markers are mitochondrial volume or membrane area. Mitochondrial protein mass is a marker frequently used for isolated mitochondria. (2) Mitochondrial marker enzymes (amounts or activities) and molecular markers can be selected as matrix markers, *e.g.*, citrate synthase activity, mtDNA or inner mt-membrane markers, *e.g.*,

cytochrome *c* oxidase activity, *aa*₃ content; TOM20. (3) Extending the measurement of mitochondrial marker enzyme activity to mitochondrial pathway capacity, measured as ETS or OXPHOS capacity, can be considered as an integrative functional mitochondrial marker.

Depending on the type of mitochondrial marker, the mitochondrial elements, *mte*, are expressed in marker-specific units. Although concentration and density are used synonymously in physical chemistry, it is recommended to distinguish *experimental mitochondrial concentration*, $C_{mte} = mte/V$ and *physiological mitochondrial density*, $D_{mte} = mte/m_X$. Then mitochondrial density is the amount of mitochondrial elements per mass of tissue. The former is mitochondrial density multiplied by sample mass concentration, $C_{mte} = D_{mte} \cdot C_{mX}$, or mitochondrial content multiplied by sample number concentration, $C_{mte} = mte_X \cdot C_{NX}$ (**Table 6**).

Mitochondria-specific flux, J_{mte,O_2} : Volume-specific metabolic O₂ flux depends on: (1) the sample concentration in the volume of the instrument chamber, C_{mX} , or C_{NX} ; (2) the mitochondrial density in the sample, $D_{mte} = mte/m_X$ or $mte_X = mte/N_X$; and (3) the specific mitochondrial activity or performance per elemental mitochondrial unit, $J_{mte,O_2} = J_{V,O_2}/C_{mte}$ (**Table 6**). Obviously, the numerical results for J_{mte,O_2} vary according to the type of mitochondrial marker chosen for measurement of *mte* and $C_{mte} = mte/V$. Some problems are common for all mitochondrial markers: (1) Accuracy of measurement is crucial, since even a highly accurate and reproducible measurement of O₂ flux becomes inaccurate and noisy if normalized for a biased and noisy measurement of a mitochondrial marker. This problem is acute in mitochondrial respiration because the denominators used (the mitochondrial marker) are often very small moieties whose accurate and precise determination is difficult. The problem is avoided when O₂ fluxes measured in substrate-uncoupler-inhibitor titration protocols are normalized for flux in a defined respiratory reference state, which is used as an *internal* marker and yields flux control ratios, *FCR* (**Fig. 7**). *FCR* are independent of any *externally* measured markers and, therefore, are statistically very robust. *FCR* indicate qualitative changes of mitochondrial respiratory con-

trol, with highest quantitative resolution, separating the effect of mitochondrial density or concentration on J_{mX,O_2} or I_{X,O_2} from that of function per elemental mitochondrial marker, J_{mte,O_2} (Pesta *et al.* 2011; Gnaiger 2014). (2) If mitochondrial quality does not change and only and only the amount of mitochondria, defined by the chosen mitochondrial marker, varies as a determinant of mass-specific flux, then any marker is equally qualified and selection of the optimum marker depends only on the accuracy and precision of measurement of the mitochondrial marker. (3) If mitochondrial flux control ratios change, then there may not be any best mitochondrial marker.

Normalization is a problematic subject and it is crucial to consider the question of the study. If the study aims to compare tissue performance, such as the effects of a certain treatment on a specific tissue, then normalization can be successful, using tissue mass or protein content, for example. If the aim, however, is to find differences of mitochondrial function independent of mitochondrial density (**Table 6**), then normalization to a mitochondrial marker is imperative. However, one cannot assume that quantitative changes in various markers such as mitochondrial proteins necessarily occur in parallel with one another. It is crucial to first establish that the marker chosen is not selectively altered by the performed treatment. In conclusion, the normalization must reflect the question at hand to reach a satisfying answer. On the other hand, the goal of comparing results across projects and institutions requires some standardization on normalization for entry into a databank.

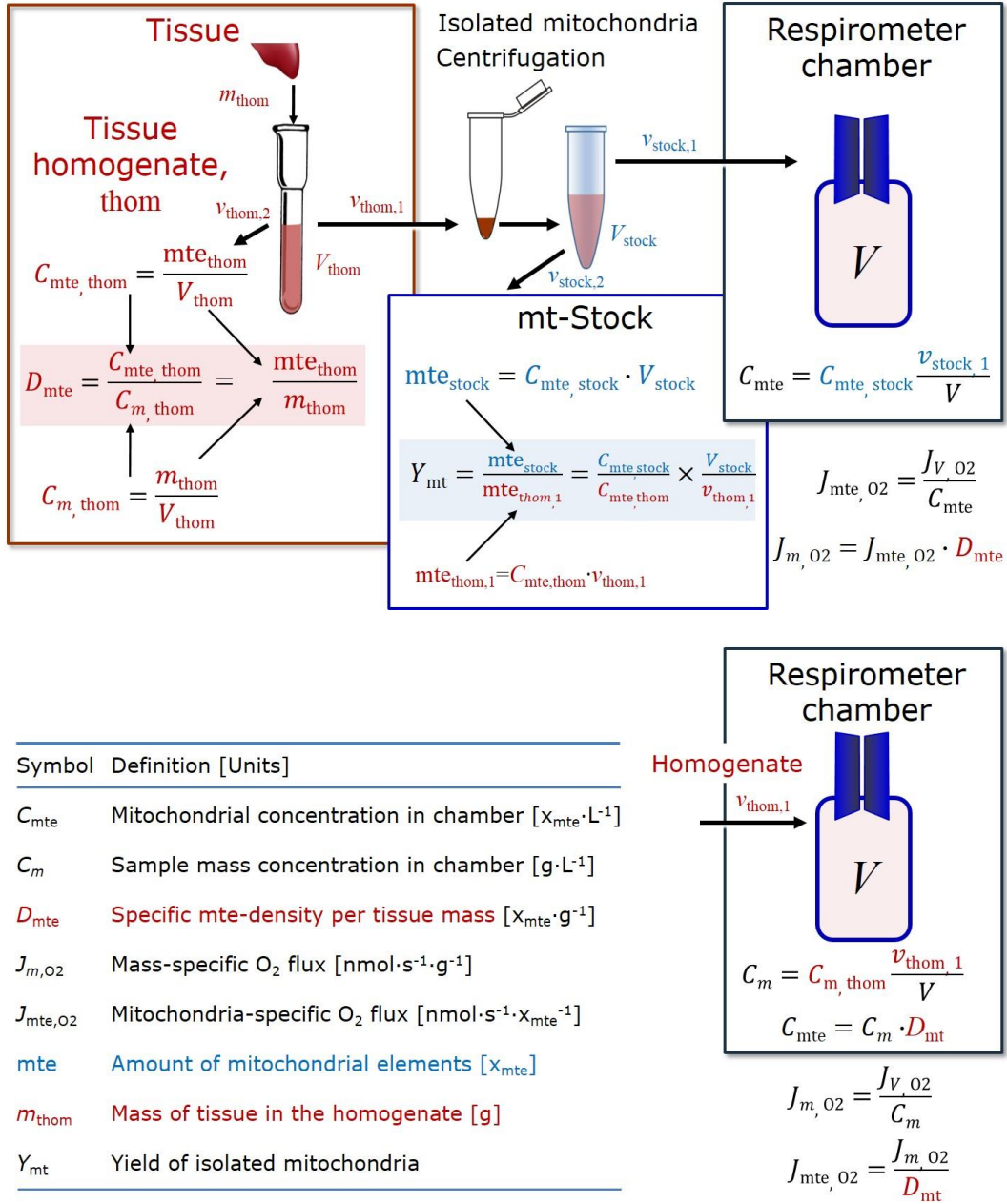


Fig. 8. Normalization of volume specific flux of isolated mitochondria and tissue homogenate. A: Mitochondrial yield, Y_{mt} , in preparation of isolated mitochondria. Specific mt-density, D_{mte} ; quantity of mt-marker, mte ; mt-concentration, C_{mte} . $v_{thom,1}$ and $v_{stock,1}$ are the volumes transferred from the total volume, V_{thom} and V_{stock} , respectively. $mte_{thom,1}$ is the amount of mitochondrial elements in volume $v_{thom,1}$ used for isolation. **B:** In respirometry with homogenate, $v_{thom,1}$ is transferred directly into the respirometer chamber. See **Table 6** for further explanation of symbols.

Table 6. Sample concentrations and normalization of flux.

| Expression | Sym- bol | Definition | Unit | Notes |
|--|---------------|--|--|-------|
| Sample | | | | |
| Identity of sample | X | Cells, animals, patients | | |
| Number of sample entities X | N_X | Number of cells, <i>etc.</i> | X | |
| Mass of sample X | m_X | | g | |
| Mass of entity X | M_X | $M_X = m_X \cdot N_X^{-1}$ | $g \cdot X^{-1}$ | |
| Mitochondria | | | | |
| Mitochondria | mt | $X=mt$ | | |
| Amount of mt-elements | mte | Quantity of mt-marker | x_{mte} | |
| Concentrations | | | | |
| Sample number concentration | C_{NX} | $C_{NX} = N_X \cdot V^{-1}$ | $X \cdot L^{-1}$ | 1 |
| Sample mass concentration | C_{mX} | $C_{mX} = m_X \cdot V^{-1}$ | $g \cdot L^{-1}$ | |
| Mitochondrial concentration | C_{mte} | $C_{mte} = mte \cdot V^{-1}$ | $x_{mte} \cdot L^{-1}$ | 2 |
| Specific mitochondrial density | D_{mte} | $D_{mte} = mte \cdot m_X^{-1}$ | $x_{mte} \cdot g^{-1}$ | 3 |
| Mitochondrial content, mte per entity X | mte_X | $mte_X = mte \cdot N_X^{-1}$ | $x_{mte} \cdot X^{-1}$ | 4 |
| O₂ flow and flux | | | | |
| Flow | I_{O_2} | Internal flow | $nmol \cdot s^{-1}$ | 5 |
| Volume-specific flux | J_{V,O_2} | $J_{V,O_2} = I_{O_2} \cdot V^{-1}$ | $nmol \cdot s^{-1} \cdot L^{-1}$ | 6 |
| Flow per sample entity X | I_{X,O_2} | $I_{X,O_2} = J_{V,O_2} \cdot C_{NX}^{-1}$ | $nmol \cdot s^{-1} \cdot X^{-1}$ | 7 |
| Mass-specific flux | J_{mX,O_2} | $J_{mX,O_2} = J_{V,O_2} \cdot C_{mX}^{-1}$ | $nmol \cdot s^{-1} \cdot g^{-1}$ | 8 |
| Mitochondria-specific flux | J_{mte,O_2} | $J_{mte,O_2} = J_{V,O_2} \cdot C_{mte}^{-1}$ | $nmol \cdot s^{-1} \cdot x_{mte}^{-1}$ | 9 |

1 In case $X=cells$, $C_{Ncell}=N_{cell} \cdot V^{-1}$ [$cell \cdot L^{-1}$]. See Table 7 for different sample types.

2 mt-concentration is an experimental variable, dependent on sample concentration: (1) $C_{mte}=mte \cdot V^{-1}$; (2) $C_{mte}=mte_X \cdot C_{NX}$; (3) $C_{mte}=C_{mX} \cdot D_{mte}$.

3 If the amount of mitochondria, mte , is expressed as mitochondrial mass, then D_{mte} is the mass fraction of mitochondria in the sample. If mte is expressed as mitochondrial volume, V_{mt} , and the mass of sample, m_X , is replaced by volume of sample, V_X , then D_{mte} is the volume fraction of mitochondria in the sample.

4 $mte_X=mte \cdot N_X^{-1}=C_{mte} \cdot C_{NX}^{-1}$.

5 Entity O_2 can be replaced by other chemical entities B to study different reactions.

6 I_{O_2} and V are defined per instrument chamber as a system of constant volume (and constant temperature), which may be closed or open. I_{O_2} is abbreviated for I_{r,O_2} , *i.e.* the metabolic or internal O_2 flow of the chemical reaction r in which O_2 is consumed, hence the negative stoichiometric number, $\nu_{O_2}=-1$. $I_{r,O_2}=d_r n_{O_2}/dt \nu_{O_2}^{-1}$. If r includes all chemical reactions in which O_2 participates, then $d_r n_{O_2} = dn_{O_2} - d_e n_{O_2}$, where dn_{O_2} is the change of the amount of O_2 in the instrument chamber and $d_e n_{O_2}$ is

the amount of O₂ added externally to the system. At steady state, by definition $d n_{O_2} = 0$, hence $d_r n_{O_2} = -d_e n_{O_2}$.

- 7 J_{V,O_2} is an experimental variable, expressed per volume of the instrument chamber.
- 8 I_{X,O_2} is a physiological variable, depending on the size of entity X.
- 9 There are many ways to normalize for a mitochondrial marker, that are used in different experimental approaches: (1) $J_{mte,O_2} = J_{V,O_2} \cdot C_{mte}^{-1}$; (2) $J_{mte,O_2} = J_{V,O_2} \cdot C_{mX}^{-1} \cdot D_{mte}^{-1} = J_{mX,O_2} \cdot D_{mte}^{-1}$; (3) $J_{mte,O_2} = J_{V,O_2} \cdot C_{NX}^{-1} \cdot mte_X^{-1} = I_{X,O_2} \cdot mte_X^{-1}$; (4) $J_{mte,O_2} = I_{O_2} \cdot mte^{-1}$.

Table 7. Some useful abbreviations of various sample types, X.

| Identity of sample | X |
|----------------------------|--------|
| Mitochondrial preparations | mtprep |
| Isolated mitochondria | imt |
| Tissue homogenate | thom |
| Permeabilized tissue | pti |
| Permeabilized fibres | pfi |
| Permeabilized cells | pce |
| Cells | ce |

4.3. Conversion: oxygen, protons, ATP

Many different units have been used to report the rate of oxygen consumption, OCR (**Tables 8 and 9**). For cellular studies we recommend that O₂ flow be expressed in units of attomole (10⁻¹⁸ mol) of O₂ consumed by each cell in a second [amol·s⁻¹·cell⁻¹], numerically equivalent to [pmol·s⁻¹·10⁻⁶ cells]. This convention allows information to be easily used when designing experiments in which oxygen consumption must be considered. For example, to estimate the volume-specific O₂ flux in an instrument chamber that would be expected at a particular cell number concentration, one simply needs to multiply the flow per cell by the number of cells per

volume of interest. This provides the amount of O₂ [mol] consumed per time [s⁻¹] per unit volume [L⁻¹]. At an O₂ flow of 100 amol·s⁻¹·cell⁻¹ and a cell density of 10⁹ cells·L⁻¹ (10⁶ cells·mL⁻¹), the volume-specific O₂ flux is 100 nmol·s⁻¹·L⁻¹ (100 pmol·s⁻¹·mL⁻¹). Because the litre is the basic unit of volume for concentration and is used for most solution chemical kinetics, if one multiplies $I_{\text{cell},\text{O}_2}$ by $C_{N\text{cell}}$, then the result will not only be the amount of O₂ [mol] consumed per time [s⁻¹] in one litre [L⁻¹], but also the change in the concentration of oxygen per second (for any volume of an ideally closed system). This is ideal for kinetic modeling as it blends with chemical rate equations where concentrations are typically expressed in mol·L⁻¹ (Wagner *et al.* 2011). Expressing O₂ consumption per cell may not be possible when dealing with tissues.

J_{O_2} is coupled in mitochondrial steady states to proton cycling, $J_{\infty\text{H}^+} = J_{\text{H}^+\text{out}} = J_{\text{H}^+\text{in}}$ (**Fig. 2**). $J_{\text{H}^+\text{out}/n}$ and $J_{\text{H}^+\text{in}/n}$ [nmol·s⁻¹·L⁻¹] are converted into electrical units, $J_{\text{H}^+\text{out}/e}$ [mC·s⁻¹·L⁻¹=mA·L⁻¹] = $J_{\text{H}^+\text{out}/n}$ [nmol·s⁻¹·L⁻¹]· F [C·mol⁻¹]·10⁻⁶ (**Table 4**). At a $J_{\text{H}^+\text{out}}/J_{\text{O}_2}$ ratio or $\text{H}^+\text{out}/\text{O}_2$ of 20 ($\text{H}^+\text{out}/\text{O}=10$), a volume-specific O₂ flux of 100 nmol·s⁻¹·L⁻¹ would correspond to a proton flux of 2,000 nmol H^+out ·s⁻¹·L⁻¹ or volume-specific current of 193 mA·L⁻¹.

$$J_{V,\text{H}^+\text{out}/e} [\text{mA}\cdot\text{L}^{-1}] = J_{V,\text{H}^+\text{out}/n} \cdot F \cdot 10^{-6} [\text{nmol}\cdot\text{s}^{-1}\cdot\text{L}^{-1}\cdot\text{mC}\cdot\text{nmol}^{-1}] \quad (\text{Eq. 10.1})$$

$$J_{V,\text{H}^+\text{out}/e} [\text{mA}\cdot\text{L}^{-1}] = J_{V,\text{O}_2} \cdot (\text{H}^+\text{out}/\text{O}_2) \cdot F \cdot 10^{-6} [\text{mC}\cdot\text{s}^{-1}\cdot\text{L}^{-1}=\text{mA}\cdot\text{L}^{-1}] \quad (\text{Eq. 10.2})$$

ETS capacity in various human cell types including HEK 293, primary HUVEC and fibroblasts ranges from 50 to 180 amol·s⁻¹·cell⁻¹, measured in intact cells in the noncoupled state (see Gnaiger 2014). At 100 amol·s⁻¹·cell⁻¹ corrected for ROX (corresponding to a catabolic power of -48 pW·cell⁻¹), the current across the mt-membranes, I_e , approximates 193 pA·cell⁻¹ or 0.2 nA per cell. See Rich (2003) for an extension of quantitative bioenergetics from the molecular to the human scale, with a transmembrane proton flux equivalent to 520 A in an adult at a catabolic power of -110 W.

Table 8. Conversion of various units used in respirometry and ergometry. e is the number of electrons or reducing equivalents. z_B is the charge number of entity B.

| 1 Unit | x | Multiplication factor | SI-Unit |
|---------------------------------------|-------------|-----------------------|------------------------------------|
| ng.atom O \cdot s $^{-1}$ | (2 e) | 0.5 | nmol O $_2$ \cdot s $^{-1}$ |
| ng.atom O \cdot min $^{-1}$ | (2 e) | 8.33 | pmol O $_2$ \cdot s $^{-1}$ |
| natom O \cdot min $^{-1}$ | (2 e) | 8.33 | pmol O $_2$ \cdot s $^{-1}$ |
| nmol O $_2$ \cdot min $^{-1}$ | (4 e) | 16.67 | pmol O $_2$ \cdot s $^{-1}$ |
| nmol O $_2$ \cdot h $^{-1}$ | (4 e) | 0.2778 | pmol O $_2$ \cdot s $^{-1}$ |
| ml O $_2$ \cdot min $^{-1}$ at STPD | | 0.744 | μ mol O $_2$ \cdot s $^{-1}$ |
| W = J/s at -470 kJ/mol O $_2$ | | -2.128 | μ mol O $_2$ \cdot s $^{-1}$ |
| mA = mC \cdot s $^{-1}$ | ($z_B=1$) | 10.36 | nmol B \cdot s $^{-1}$ |
| nmol B \cdot s $^{-1}$ | ($z_B=1$) | 0.09649 | mA |

Table 9. Conversion for units with preservation of numerical values. For prefixes see Table 10.

| Name | Frequently used unit | Equivalent unit |
|-----------------------------------|---|---|
| Volume-specific flux, J_{V,O_2} | pmol \cdot s $^{-1}$ \cdot mL $^{-1}$ | nmol \cdot s $^{-1}$ \cdot L $^{-1}$ |
| | mol \cdot s $^{-1}$ \cdot m $^{-3}$ | mmol \cdot s $^{-1}$ \cdot L $^{-1}$ |
| Cell-specific flow, I_{O_2} | pmol \cdot s $^{-1}$ \cdot 10 $^{-6}$ cells | amol \cdot s $^{-1}$ \cdot cell $^{-1}$ |
| Cell density, C_{ce} | 10 6 cells \cdot mL $^{-1}$ | 10 9 cells \cdot L $^{-1}$ |
| Mass-specific flux, J_{m,O_2} | pmol \cdot s $^{-1}$ \cdot mg $^{-1}$ | nmol \cdot s $^{-1}$ \cdot g $^{-1}$ |
| Catabolic power, P_{k,O_2} | μ W \cdot 10 $^{-6}$ cells | pW \cdot cell $^{-1}$ |
| Volume | L | dm 3 |
| | mL | cm 3 |
| Amount of substance concentration | M = mol \cdot L $^{-1}$ | mol \cdot dm $^{-3}$ |

For NADH- and succinate-linked respiration, the mechanistic »P/O $_2$ ratio (referring to the full 4 electron reduction of O $_2$) is calculated at 20/3.7 and 12/3.7, respectively (Eq. 11) equal to 5.4 and 3.3. The classical »P/O ratios (referring to the 2 electron reduction of 0.5 O $_2$) are 2.7 and 1.6 (Watt *et al.* 2010), in direct agreement with the measured »P/O ratio for succinate of 1.58 \pm 0.02 (Gnaiger *et al.* 2000; for detailed reviews see Wikström and Hummer 2012; Sazanov 2015),

$$\text{»P/O}_2 = (\text{H}^+_{\text{out}}/\text{O}_2)/(\text{H}^+_{\text{in}}/\text{»P}) \quad (11)$$

In summary (**Fig. 1**),

$$J_{V, \gg P} [\text{nmol} \cdot \text{s}^{-1} \cdot \text{L}^{-1}] = J_{V, \text{O}_2} \cdot (\text{H}^+_{\text{out}} / \text{O}_2) / (\text{H}^+_{\text{in}} / \gg P) \quad (12.1)$$

$$J_{V, \gg P} [\text{nmol} \cdot \text{s}^{-1} \cdot \text{L}^{-1}] = J_{V, \text{O}_2} \cdot (\gg P / \text{O}_2) \quad (12.2)$$

Considering isolated mitochondria as powerhouses and proton pumps as molecular machines and relating the experimental results to energy metabolism of the intact cell, the cellular $\gg P / \text{O}_2$ based on oxidation of glycogen is increased by the glycolytic substrate-level phosphorylation of 3 $\gg P / \text{Glyc}$, *i.e.*, 0.5 mol $\gg P$ for each mol O_2 consumed in the complete oxidation of a mol glycosyl unit (Glyc). Adding 0.5 to the mitochondrial $\gg P / \text{O}_2$ ratio of 5.4 yields a bioenergetic cell physiological $\gg P / \text{O}_2$ ratio close to 6. Two NADH equivalents are formed during glycolysis and transported from the cytosol into the mitochondrial matrix, either by the malate-aspartate shuttle or by the glycerophosphate shuttle resulting in different theoretical yield of ATP generated by mitochondria, the energetic cost of which potentially must be taken into account. Considering also substrate-level phosphorylation in the TCA cycle, this high $\gg P / \text{O}_2$ ratio not only reflects proton translocation and OXPHOS studied in isolation, but integrates mitochondrial physiology with energy transformation in the living cell (Gnaiger 1993b).

5. Conclusions

MitoEAGLE can serve as a gateway to better diagnose mitochondrial respiratory defects linked to genetic variations, age-related health risks, gender-specific mitochondrial performance, life style with its effects on degenerative diseases, and environmental exposure to thermal regimes and chemical compounds. The present recommendations on coupling control (Part 1) will be extended in a series of manuscripts on pathway control of mitochondrial respiration, respiratory states in intact cells, and harmonization of experimental procedures.

The optimal choice for expressing O_2 flow per biological system, and normalization for specific tissue-markers (volume, mass, protein) and mitochondrial markers (volume, protein, content, mtDNA, activity of marker enzymes, respiratory reference state) is guided by the sci-

entific question. Interpretation of the obtained data depends critically on appropriate normalization, and therefore reporting rates merely as $\text{nmol}\cdot\text{s}^{-1}$ is discouraged, since it restricts the analysis to intra-experimental comparison of relative (qualitative) differences. For studies with intact or permeabilized cells, we recommend that normalizations be provided as far as possible: (1) on a per cell basis as O_2 flow (a biophysical normalization); (2) per g cell protein or per cell mass as mass-specific O_2 flux (a cellular normalization); and (3) per mitochondrial marker as mt-specific flux (a mitochondrial normalization). With information on cell size and the use of both normalizations, maximum potential information is available (Renner *et al.* 2003; Wagner *et al.* 2011; Gnaiger 2014). When using isolated mitochondria, mitochondrial protein is a frequently applied mitochondrial marker, the use of which is basically restricted to isolated mitochondria. Mitochondrial markers, such as citrate synthase activity as an enzymatic matrix marker, provide a link to the tissue of origin on the basis of calculating the mitochondrial yield, *i.e.*, the fraction of mitochondrial marker obtained from a unit mass of tissue.

For an overall perspective of mitochondrial physiology, we may link cellular bioenergetics to systemic human respiratory activity, addressing cell- and tissue-specific mitochondrial function as the next step. An O_2 flow of $234 \mu\text{mol}\cdot\text{s}^{-1}$ per individual or flux of $3.3 \text{ nmol}\cdot\text{s}^{-1}\cdot\text{g}^{-1}$ body mass corresponds to -110 W catabolic energy flow at a body mass of 70 kg and -470 kJ/mol O_2 . Considering a cell count of $514\cdot 10^6$ cells per g tissue mass (Ahluwalia 2017), the average O_2 flow per cell at $J_{m,\text{O}_2\text{peak}}$ of $45 \text{ nmol}\cdot\text{s}^{-1}\cdot\text{g}^{-1}$ ($60 \text{ mL O}_2\cdot\text{min}^{-1}\cdot\text{kg}^{-1}$) is $88 \text{ amol}\cdot\text{s}^{-1}\cdot\text{cell}^{-1}$, which compares well with OXPHOS capacity of human fibroblasts (not ETS but the lower OXPHOS capacity is used as a reference; Gnaiger 2014). We can describe our bodies as the sum of $37\cdot 10^{12}$ cells (37 trillion cells; Bianconi 2013). An estimate of mitochondrial content at 300 mitochondria per cell (West *et al.* 2002) raises questions on the concept of mitochondrial number (**Table 9**). Mitochondrial fitness of our $11\cdot 10^{15}$ mitochondria (11 quadrillion mt) is indicated if O_2 flow of $0.02 \text{ amol}\cdot\text{s}^{-1}\cdot\text{mt}^{-1}$ at rest can be activated to $0.3 \text{ amol}\cdot\text{s}^{-1}\cdot\text{mt}^{-1}$ at high ergometric performance.

Acknowledgements

Supported by COST Action CA15203 MitoEAGLE and K-Regio project MitoFit (EG).

Competing financial interests: E.G. is founder and CEO of Oroboros Instruments, Innsbruck, Austria.

6. References *(incomplete; www links will be deleted in the final version)*

Ahluwalia A. Allometric scaling in-vitro. *Sci Rep* 2017;7:42113.

Altmann R. Die Elementarorganismen und ihre Beziehungen zu den Zellen. Zweite vermehrte Auflage. Verlag Von Veit & Comp, Leipzig 1894;160 pp. - www.mitoeagle.org/index.php/Altmann_1894_Verlag_Von_Veit_%26_Comp

Bianconi E, Piovesan A, Facchin F, Beraudi A, Casadei R, Frabetti F, Vitale L, Pelleri MC, Tassani S, Piva F, Perez-Amodio S, Strippoli P, Canaider S. (2013) An estimation of the number of cells in the human body. *Ann Hum Biol* 40:463-71. - <http://dx.doi.org/10.3109/03014460.2013.807878> PMID: 23829164

Birkedal R, Laasmaa M, Vendelin M. The location of energetic compartments affects energetic communication in cardiomyocytes. *Front Physiol* 2014;5:376. doi: 10.3389/fphys.2014.00376. eCollection 2014. PMID: 25324784

Brown GC. Control of respiration and ATP synthesis in mammalian mitochondria and cells. *Biochem J* 1992;284:1-13. - www.mitoeagle.org/index.php/Brown_1992_Biochem_J

Chance B, Williams GR. Respiratory enzymes in oxidative phosphorylation: III. The steady state. *J Biol Chem* 1955;217:409-27. - www.mitoeagle.org/index.php/Chance_1955_J_Biol_Chem-III

Chance B, Williams GR. Respiratory enzymes in oxidative phosphorylation. IV. The respiratory chain. *J Biol Chem* 1955;217:429-38. - www.mitoeagle.org/index.php/Chance_1955_J_Biol_Chem-IV

Chance B, Williams GR. The respiratory chain and oxidative phosphorylation. *Adv Enzymol*

Relat Subj Biochem 1956;17:65-134. - www.mitoeagle.org/index.php/Chance_1956_Adv_Enzymol_Relat_Subj_Biochem

Cohen ER, Cvitas T, Frey JG, Holmström B, Kuchitsu K, Marquardt R, Mills I, Pavese F, Quack M, Stohner J, Strauss HL, Takami M, Thor HL. Quantities, Units and Symbols in Physical Chemistry, IUPAC Green Book 2008;3rd Edition, 2nd Printing, IUPAC &

RSC Publishing, Cambridge. - www.mitoeagle.org/index.php/Cohen_2008_IUPAC_Green_Book

Coopersmith J. Energy, the subtle concept. The discovery of Feynman's blocks from Leibnitz to Einstein. Oxford University Press 2010;400 pp.

Dufour S, Rousse N, Canioni P, Diolez P. Top-down control analysis of temperature effect on oxidative phosphorylation. *Biochem J* 1996;314:743-51.

Ernster L, Schatz G Mitochondria: a historical review. *J Cell Biol* 1981;91:227s-55s. - www.mitoeagle.org/index.php/Ernster_1981_J_Cell_Biol

Estabrook RW. Mitochondrial respiratory control and the polarographic measurement of ADP:O ratios. *Methods Enzymol* 1967;10:41-7. - www.mitoeagle.org/index.php/Estabrook_1967_Methods_Enzymol

Fell D. Understanding the control of metabolism. Portland Press 1997.

Garlid KD, Semrad C, Zinchenko V. Does redox slip contribute significantly to mitochondrial respiration? In: Schuster S, Rigoulet M, Ouhabi R, Mazat J-P (eds) *Modern trends in biothermokinetics*. Plenum Press, New York, London 1993;287-93.

Gnaiger E. Efficiency and power strategies under hypoxia. Is low efficiency at high glycolytic ATP production a paradox? In: *Surviving Hypoxia: Mechanisms of Control and Adaptation*. Hochachka PW, Lutz PL, Sick T, Rosenthal M, Van den Thillart G (eds.) CRC Press, Boca Raton, Ann Arbor, London, Tokyo 1993a:77-109. -

www.mitoeagle.org/index.php/Gnaiger_1993_Hypoxia

- Gnaiger E. Nonequilibrium thermodynamics of energy transformations. Pure Appl Chem 1993b;65:1983-2002. - www.mitoeagle.org/index.php/Gnaiger_1993_Pure_Appl_Chem
- Gnaiger E. Bioenergetics at low oxygen: dependence of respiration and phosphorylation on oxygen and adenosine diphosphate supply. Respir Physiol 2001;128:277-97. - www.mitoeagle.org/index.php/Gnaiger_2001_Respir_Physiol
- Gnaiger E. Mitochondrial pathways and respiratory control. An introduction to OXPHOS analysis. 4th ed. Mitochondr Physiol Network 2014;19.12. Oroboros MiPNet Publications, Innsbruck:80 pp. - www.mitoeagle.org/index.php/Gnaiger_2014_MitoPathways
- Gnaiger E. Capacity of oxidative phosphorylation in human skeletal muscle. New perspectives of mitochondrial physiology. Int J Biochem Cell Biol 2009;41:1837-45. - www.mitoeagle.org/index.php/Gnaiger_2009_Int_J_Biochem_Cell_Biol
- Gnaiger E, Méndez G, Hand SC. High phosphorylation efficiency and depression of uncoupled respiration in mitochondria under hypoxia. Proc Natl Acad Sci USA 2000;97:11080-5. - www.mitoeagle.org/index.php/Gnaiger_2000_Proc_Natl_Acad_Sci_U_S_A
- Hofstadter DR. Gödel, Escher, Bach: An eternal golden braid. A metaphorical fugue on minds and machines in the spirit of Lewis Carroll. Harvester Press 1979;499 pp. - www.mitoeagle.org/index.php/Hofstadter_1979_Harvester_Press
- Illaste A, Laasmaa M, Peterson P, Vendelin M. Analysis of molecular movement reveals latticelike obstructions to diffusion in heart muscle cells. Biophys J 2012;102:739-48. - PMID: 22385844
- Jepihhina N, Beraud N, Sepp M, Birkedal R, Vendelin M. Permeabilized rat cardiomyocyte response demonstrates intracellular origin of diffusion obstacles. Biophys J 2011;101:2112-21. - PMID: 22067148

- Komlódi T, Tretter L. Methylene blue stimulates substrate-level phosphorylation catalysed by succinyl-CoA ligase in the citric acid cycle. *Neuropharmacology* 2017;123:287-98. - www.mitoeagle.org/index.php/Komlodi_2017_Neuropharmacology
- Lemieux H, Blier PU, Gnaiger E. Remodeling pathway control of mitochondrial respiratory capacity by temperature in mouse heart: electron flow through the Q-junction in permeabilized fibers. *Sci Rep* 2017;7:2840. - www.mitoeagle.org/index.php/Lemieux_2017_Sci_Rep
- Miller GA. *The science of words*. Scientific American Library New York 1991;276 pp. - www.mitoeagle.org/index.php/Miller_1991_Scientific_American_Library
- Mitchell P. Chemiosmotic coupling in oxidative and photosynthetic phosphorylation *Biochim Biophys Acta Bioenergetics* 2011;1807:1507-38. - <http://www.sciencedirect.com/science/article/pii/S0005272811002283>
- Mitchell P, Moyle J. Respiration-driven proton translocation in rat liver mitochondria. *Biochem J* 1967;105:1147-62. - www.mitoeagle.org/index.php/Mitchell_1967_Biochem_J
- Morrow RM, Picard M, Derbeneva O, Leipzig J, McManus MJ, Gouspillou G, Barbat-Artigas S, Dos Santos C, Hepple RT, Murdock DG, Wallace DC. Mitochondrial energy deficiency leads to hyperproliferation of skeletal muscle mitochondria and enhanced insulin sensitivity. *Proc Natl Acad Sci U S A* 2017;114:2705-10. - www.mitoeagle.org/index.php/Morrow_2017_Proc_Natl_Acad_Sci_U_S_A
- Nicholls DG, Ferguson S. *Bioenergetics 4*. Elsevier 2013.
- Prigogine I. *Introduction to thermodynamics of irreversible processes*. Interscience, New York, 1967;3rd ed.
- Puchowicz MA, Varnes ME, Cohen BH, Friedman NR, Kerr DS, Hoppel CL. Oxidative phosphorylation analysis: assessing the integrated functional activity of human skeletal muscle mitochondria – case studies. *Mitochondrion* 2004;4:377-85. - www.mitoeagle.org/index.php/Puchowicz_2004_Mitochondrion

- Renner K, Amberger A, Konwalinka G, Gnaiger E. Changes of mitochondrial respiration, mitochondrial content and cell size after induction of apoptosis in leukemia cells. *Biochim Biophys Acta* 2003;1642:115-23. - www.mitoeagle.org/index.php/Renner_2003_Biochim_Biophys_Acta
- Rich P. Chemiosmotic coupling: The cost of living. *Nature* 2003;421:583. - www.mitoeagle.org/index.php/Rich_2003_Nature
- Rostovtseva TK, Sheldon KL, Hassanzadeh E, Monge C, Saks V, Bezrukov SM, Sackett DL. Tubulin binding blocks mitochondrial voltage-dependent anion channel and regulates respiration. *Proc Natl Acad Sci USA* 2008;105:18746-51. - www.mitoeagle.org/index.php/Rostovtseva_2008_Proc_Natl_Acad_Sci_U_S_A
- Rustin P, Parfait B, Chretien D, Bourgeron T, Djouadi F, Bastin J, Rötig A, Munnich A. Fluxes of nicotinamide adenine dinucleotides through mitochondrial membranes in human cultured cells. *J Biol Chem* 1996;271:14785-90.
- Saks VA, Veksler VI, Kuznetsov AV, Kay L, Sikk P, Tiivel T, Tranqui L, Olivares J, Winkler K, Wiedemann F, Kunz WS. Permeabilised cell and skinned fiber techniques in studies of mitochondrial function in vivo. *Mol Cell Biochem* 1998;184:81-100. - http://www.mitoeagle.org/index.php/Saks_1998_Mol_Cell_Biochem
- Sazanov LA. A giant molecular proton pump: structure and mechanism of respiratory complex I. *Nat Rev Mol Cell Biol* 2015;16:375-88. - www.mitoeagle.org/index.php/Sazanov_2015_Nat_Rev_Mol_Cell_Biol
- Schrödinger E. *What is life? The physical aspect of the living cell*. Cambridge Univ Press, 1944. - www.mitoeagle.org/index.php/Gnaiger_1994_BTK
- Simson P, Jepihhina N, Laasmaa M, Peterson P, Birkedal R, Vendelin M. Restricted ADP movement in cardiomyocytes: Cytosolic diffusion obstacles are complemented with a small number of open mitochondrial voltage-dependent anion channels. *J Mol Cell Cardiol* 2016;97:197-203. - PMID: 27261153

- Stucki JW, Ineichen EA. Energy dissipation by calcium recycling and the efficiency of calcium transport in rat-liver mitochondria. *Eur J Biochem* 1974;48:365-75.
- Wagner BA, Venkataraman S, Buettner GR. The rate of oxygen utilization by cells. *Free Radic Biol Med*. 2011;51:700-712.
<http://dx.doi.org/10.1016/j.freeradbiomed.2011.05.024> PMID: PMC3147247
- Watt IN, Montgomery MG, Runswick MJ, Leslie AG, Walker JE. Bioenergetic cost of making an adenosine triphosphate molecule in animal mitochondria. *Proc Natl Acad Sci U S A* 2010;107:16823-7. - www.mitoeagle.org/index.php/Watt_2010_Proc_Natl_Acad_Sci_U_S_A
- Weibel ER, Hoppeler H. Exercise-induced maximal metabolic rate scales with muscle aerobic capacity. *J Exp Biol* 2005;208:1635–44.
- West GB, Woodruff WH, Brown JH. Allometric scaling of metabolic rate from molecules and mitochondria to cells and mammals. *Proc Natl Acad Sci USA* 2002;99 Suppl 1:2473–8.
- Wikström M, Hummer G. Stoichiometry of proton translocation by respiratory complex I and its mechanistic implications. *Proc Natl Acad Sci U S A* 2012;109:4431-6. - www.mitoeagle.org/index.php/Wikstroem_2012_Proc_Natl_Acad_Sci_U_S_A